BRNO UNIVERSITY OF TECHNOLOGY

VYSOKÉ UČENÍ TECHNICKÉ V BRNĚ

CENTRAL EUROPEAN INSTITUTE OF TECHNOLOGY BUT

STŘEDOEVROPSKÝ TECHNOLOGICKÝ INSTITUT VUT

NEW TECHNIQUE ON A CHIP FOR RAPID DETECTION OF BIOLOGICAL MATERIALS

NOVÉ METODY PRO RYCHLOU DETEKCI BIOLOGICKÉHO MATERIÁLU NA ČIPU

DOCTORAL THESIS
DIZERTAČNÍ PRÁCE

AUTHOR — **Jelena Pejovič Simeunovič**
AUTOR PRÁCE

SUPERVISOR — **doc. Ing. Jaromír Hubálek, Ph.D.**
ŠKOLITEL

BRNO 2020

ABSTRACT

This work proposes a technique for on-chip separation and detection of quantum dots (QDs) conjugated with various proteins in order to study the influence of the coupling agent on a quenching of QD fluorescence intensity caused by conjugation to a protein and to perform multi-analyte immunoassay to identify small amounts of the protein. Under optimal conditions, bioconjugated QDs were successfully separated from free QDs within 10 minutes. Particles and target solutions were mixed, and on-chip detection was performed using a device developed in our laboratory. Only one excitation light source was used in combination with several filters for different emission wavelengths. Fluorescence emitted by the two types of conjugated QDs could then be recorded simultaneously since the QDs emitted light at different wavelengths while being excited at the same wavelength. By mixing two types of QDs bioconjugated with two kinds of proteins and antibodies we were able to detect immunocomplex peaks with varying areas. The peak area depended on concentration of QDs and antigens, on the progress of antibody-antigen reaction and proved to be linearly correlated with the antigen concentration. We showed that on-chip capillary electrophoresis of QDs can be used as a sensitive technique for detection of biological molecules. The main benefits of this method are simplicity, small sample and reagent volume requirements, and high efficiency of separation.

ABSTRAKT

Tato práce navrhuje techniku separace a detekce na čipu pro kvantové tečky (QD, „quantum dots“) konjugované s různými proteiny, za účelem sledování vlivu vazebného činidla na potlačení intenzity fluorescence QD způsobené konjugací s proteinem a za účelem provedení multianalytické imunoanalýzy k identifikaci malých množství daného proteinu. Za optimálních podmínek byly biokonjugované QD úspěšně odděleny od těch nezkonjugovaných během 10 minut. Částice a cílové roztoky byly smíchány a detekce na čipu byla provedena za pomoci zařízení vyvinutého v naší laboratoři. Byl použit pouze jeden zdroj excitačního světla v kombinaci s několika filtry pro různé emisní vlnové délky. Fluorescence emitovaná dvěma typy konjugovaných QD mohla být poté zaznamenána současně, protože QD emitovaly světlo na různých vlnových délkách, ačkoliv byly excitovány při stejné vlnové délce. Smícháním dvou typů QD biokonjugovaných se dvěma druhy proteinů a protilátek jsme dokázali detekovat imunokomplexní píky s různými plochami. Plocha pod píkem závisela na koncentraci QD a antigenů, na postupu reakcí protilátka–antigen a ukázalo se, že je lineárně korelována s koncentrací antigenu. Ukázali jsme, že kapilární elektroforéza QD na čipu může být použita jako citlivá technika pro detekci biologických molekul. Hlavními výhodami této metody jsou jednoduchost, malé požadavky na objem vzorku i činidla a také vysoká účinnost separace.

KEY WORDS: quantum dots, bioconjugation, capillary electrophoresis, immunoassays, fluorescence quenching

KLÍČOVÁ SLOVA: kvantové tečky, biokonjugace, kapilární elektroforéza, imunoanalytické systémy, zhášení fluorescence

BIBLIOGRAPHIC CITATION:

PEJOVIČ SIMEUNOVIČ, Jelena. New technique on a chip for rapid detection of biological materials. Brno, 2020. Dostupné také z: https://www.vutbr.cz/studenti/zav-prace/detail/125713. Doctoral Thesis. Vysoké učení technické v Brně, Středoevropský technologický institut VUT, Central European Institute of Technology BUT. Supervisor Jaromír Hubálek.

DECLARATION

I certify that the work presented in this thesis was performed independently, under the supervision of doc.Ing. Jaromír Hubálek Ph.D., and is original with the sole exception of the technical literature and other sources of information that are acknowledged in the text and reference list, and that the material has not been submitted, in whole or in part, for a degree at this or any other university.

Brno . . . .

(author's signature)

ACKNOWLEDGEMENTS

I would like to thank to my supervisor doc. Ing. Jaromír Hubálek, Ph.D. for accepting me in the group and for his valuable advices, technical and pedagogical support and patient during my studies. Also, I would like to thank to all my colleagues (past and present) from the group Smart Nanodevice at CEITEC VUT for their cooperation, professionalisms, lessons and suggestions not only academic but also from day-to-day life. Special gratitude goes to prof. Ing. Pavel Neužil, Dr., DSc. for his innovative ideas, discussions and technical advices.

My thesis is a result of several collaborations. I was fortune enough to spend eight months in Department of Nanobiotechnology at University of Natural Resources and Life Sciences in Vienna. Special gratitude goes to Univ. Prof. Dr. Erik Reimhult for his enthusiasm in research and optimism when facing dilemma. Big piece of collaborative effort was the work on a chip electrophoresis immunoassay for multiple antibodies which was done with professor Mirek Macka from School of Natural Sciences and Australian Centre for Research on Separation Science (ACROSS), University of Tasmania, whom I thank for his energy, clear vision and great knowledge that he was willing to share, and doc. Mgr. Markéta Vaculovičová, Ph.D., form Department of Chemistry and Biochemistry, Mendel University in Brno, whom I thank for being extremely generous with sharing her knowledge, lab equipment, and experimental materials.

My sincere gratitude goes to my family and friends. My friends for being there whenever I need them the most and for enjoyable distractions of my studies. My brother and mother for their support and encouragement and my husband for his love, trust and patient. Last, but not least I dedicate this work to Vuk and Lazar my biggest inspiration.

TABLE OF CONTENTS

1. INTRODUCTION

The aim of this PhD thesis is to develop and test chip-based technique, for separation and detection of different biological material. The work presented in this thesis is concentrate on using lab on a chip (LOC) technology to detect and separate quantum dots (QDs) and bioconjugated QDs using capillary electrophoresis (CE) on a chip, as well as screen and detect multiple analytes with minimal sample processing and handling using CE immunoassay.

Due to development in medicine, chemistry, drug discovery, environmental industry, and other industries world has become very dependent on a (bio) chemical analysis. To preform chemical analysis in traditional way we need to have certain amount of sample (water, blood…), modern equipment in laboratories and skilled people to perform demanding procedures. All this steps are time, energy and money consuming. New trend in technology moves towards performing few laboratory functions on one device, so called LOC technology.

Performing analysis with this technology is much easier and available to individuals with no special training and skills. Aim of this technology is to make small, portable device, easy to use. This goal equipment should be smaller, portable, easier to operate and reliable. LOC technology represent all this steps required for an analysis on a miniaturized system.

One of the most important components of the LOC device is the chip in which sample of micro- and nanoliters and reagents are moved around with very high accuracy. By dramatically reducing amount of samples and regents used, LOC offers a significant decrease in the cost. Since LOC technology is closely related and overlap with microfluidics, part of physics that examines properties of fluid in micro and nano-scale, it is important to understand behavior of fluid in microscale to be able to fabricate functionalized device used in different application.

Quantum dots (QDs) are nanoparticles (NPs) composed of periodic groups of III–V or II–VI semiconductor materials such as ZnS, ZnSe, CdS, CdSe, CdTe, and others [1] . Their unique optical and electronic properties placed them between those of bulk materials and isolated molecules of atoms [2]. Due to their remarkable properties, such as high quantum yield, large Stokes shift, broad absorption spectra, long fluorescent lifetimes, size-tunable photoluminescent emissions, and low levels of photobleaching, QDs are very attractive candidates for use in biolabeling, biological assay, and imaging [3]. However, the core of QDs created with heavy metals such as cadmium and lead are toxic for living systems and cells. To address these issues, numerous studies have centered on the development of QDs composed of materials with reduced toxicity, such as carbon (including graphene-like), silicon, and I–III–IV semiconductors (Ag_2S, Ag_2Te) and others [4]. To enhance QDs solubility under physiological condition and reduce their toxicity, a lot of research has also been addressed to surface coating of QDs [5]. Even, these modified QDs bring doubts [6], and more research needs to be done to investigate QDs and their bioconjugation.

QDs were conjugated to proteins [7-9], antibodies [10-12], enzymes [13], DNA [14], and peptides [15] to could be used in wide range of biological application [16]. There are mainly two strategies to conjugate QDs to a biomolecule: electrostatic interaction and covalent conjugation. Conjugation based on electrostatic interaction is easier to operate but not stable, while covalent conjugation uses coupling agents which by modification of QD surface makes very stable complex [17]. So-called zero-length-cross-linking agents are mostly used as coupling agents, such as carbonyldiimidazole (CDI), 1-ethyl-3-(3-dimethylaminopropyl)carbodiimide (EDC), or two-step procedure combining EDC with N-hydroxysulfosuccinimide (sulfo-NHS), that conjugate carboxyl groups and amines to form stable covalent amide linkages [18].

CE has emerged as a powerful tool for separation and characterizing of mixtures used for instance in HPLC technique. In recent 10 years, separating QDs and other NPs [19, 20] is under the study and using in analytics is highly promising. On-a-chip electrophoresis has some advantages over the conventional one, since it requires low sample volume, fast separation time, and high separation efficiencies, and in addition, microchip platform provides the possibility to integrate sampling, separation, and detection on a chip [21].

Immunoassay is a type of a protein assay based on the immunoreaction between an antibody and antigen. High selectivity and strong nature of antibody-antigen interactions makes antibodies or related agents valuable as reagents for the measurement and detection of analytes in complex samples such as blood, plasma, serum, urine, tissue sample [22]. Most immunoassays are conventionally carried out using a microplate. However, bulk-scale assays often require long analysis times and large amounts of sample/reagents. Moreover, labor-intensive manipulations are required to mix the solutions for the immunoreaction, separate the free antibody from the antigen-antibody complex (bound/free (B/F) separation) for selective assays, with low background signals. In enzyme-linked immunosorbent assay (ELISA) [23], further sensitive detection can be achieved by using an enzyme-labeled secondary antibody and its substrate, but it needs a longer analysis time and complex procedures. To overcome these drawbacks, immunoassay methods based on microfluidic devices have been developed recently [24-26]. Many types of immunoassays involve some form of a separation step for examining either the various species that may contain a label or for separating the bound and non-bound forms of a labeled species form each other. CE as a separation component in immunoassays has been used widely [27, 28]. Microfluidic devices based on a CE offer several advantages such as rapid reactions due to a short length for diffusion, effective reactions due to high surface/volume ratio, and minimal consumption of samples and reagents. These microfluidic techniques enabled rapid immunoassays with minimal consumption of reagents and samples, although the difficulty in the fabrication of these devices remains a problem. Thus, the running costs of immunoassays have not been reduced markedly by the above-mentioned reported microfluidic assays. In our work we used Polydimethylsiloxane (PDMS) chip to perform on a chip CE proof concept immunoassay, to reduce the price of fabrication of a device.

The fluorescent immunoassays have gained popularity due to their sensitivity, diverse selection of fluorophores, easy operation and various readout modes [29]. Even though,

several multiplexed dye-based assays have been reported in literature [30, 31], their narrow absorption and broad tailed emission spectra caused problems, such as cross-signaling, poor emission and undesired loss of photoluminescence signal [32]. A variety of inorganic nanocrystals have been designed, synthesized, and functionalized, with the aim of utilizing their unique nanoscale properties to either improve existing biosensing methods or to develop new sensing strategies [33].

Detection of multiple biomarkers has recently received a great interest from biosensors community. The ability of multiplexed detection of biomolecules is the key in order to accelerate the advances in genomics, proteomics, and disease prevention. These diagnostic methods must be rapid, specific, sensitive and cost-effective.

Taking in consideration everything above and scientific importance for solving problems in bioconjugation of QDs and their separation and detection with on a chip platforms, aim of this thesis is on one side to investigate bonding between QDs and biomolecules and on the other side to detect multiple biomolecules using CE immunoassay.

We used a simple method to monitor the formation of protein–QD complex based on mobility changes. Detection and separation of BSA–QD conjugates were done in microfluidic system, with on-a-chip electrophoresis and optical detection. QDs and QD–protein conjugates were successfully separated using on-a-chip CE within 10 min. Conjugation of QDs with BSA was achieved via covalent coupling. FL-quenching efficiency and the aspect of quenching mechanism of QDs bounded with BSA were studied by FL spectroscopy. The results present that BSA can effectively quench FL of QDs, which could be explained by a covalent interaction between the NPs and the quencher (protein), demonstrating the formation of QD–BSA bioconjugates. The highest quenching effect was notable when EDC/sulfo-NHS is used as a crosslinker.

The following two proteins were selected for this study: bovine serum albumin (BSA) and mouse immunoglobulin G (mIgG). These model proteins were chosen with respect to the reliable, specific and selective immunoreactivity with appropriate antibodies exhibiting low cross-reactivity. Moreover, significantly different properties (molecular mass and pI) ensure optimal electrophoretic behavior for development and optimization of the method.

Developing of rapid, sensitive and reliable assay of bioanalytes is highly important in various industries including food, healthcare, pharmacy, etc. [1]. A method combining high selectivity of immunochemical reaction with the separation efficiency of CE was used to monitor the formation of QD-labeled immunocomplex based on electrophoretic mobility changes. Moreover the influence of antigen and QDs concentration on separation performance was studied. Using one excitation wavelength and two types of filter set up it was possible to detect two different immunocomplexes simultaneously.

Together, both QDs and CE on a chip can be applied as a sensitive technique for the detection of biological molecules. This method has the ability to screen and detect multiple analytes with minimal sample processing and handling.

2. AIMS OF THE THESIS

Taking in consideration scientific importance for solving problems in bioconjugation of QDs and their separation and detection with on a chip platforms, aim of this thesis is to seek for best bonding technique between QDs and biomolecules and to detect multiple biomolecules using CE immunoassay. This aim can be divided into few objectives to be solved:

1. Choosing and testing suitable procedure for synthesis of QDs
2. Propose the appropriate strategy for conjugation of QDs with biological molecule
3. Evaluate performance of the proposed conjugation techniques
4. Developing in our laboratory electro-optical system for the separation and fluorescence detection of bioconjugated QDs
5. Studying of QDs luminescence quenching effect caused by covalent conjugation with protein using on a chip CE
6. Evaluate performance of electro-optical system on a chip using a multi-analyte immunoassay based on quantum dots (QDs) fluorescence

3. EXPERIMENTAL METHODS

3.1 Synthesis of CdTe QDs capped with MPA

The procedure for synthesis of MPA-capped CdTe QDs was adapted from the work of Long *et al.* [34]. $CdCl_2$ (183 mg) and 400 mg trisodium citrate were dissolved in 90 cm^3 of water, followed by the addition of 104 mm^3 of MPA. The pH of the solution was adjusted to 10 using 1 mol dm^{-3} NaOH. 44 mg of Na_2TeO_3 and 100 mg of $NaBH_4$ were added to the solution under vigorous stirring. The mixture was kept at 95 °C under the reflux cooling (Figure 1) a specific time (depending on the size of QD that we expected to achieve) for 1 and 2 hours for green and orange respectively.

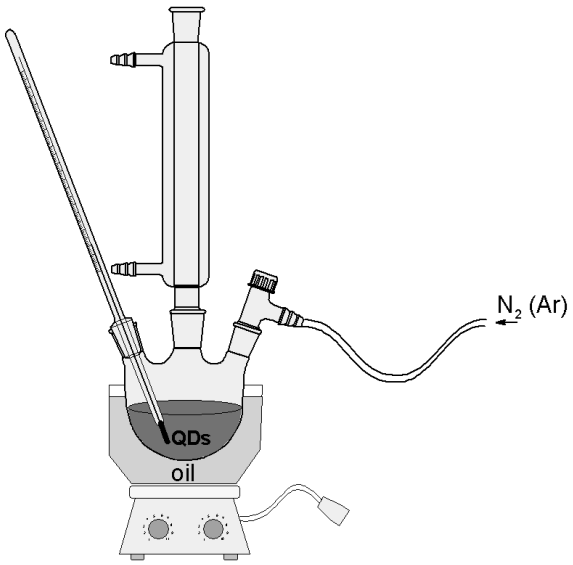

Figure 1 Schema of apparatus for QDs preparation in reflux condenser

3.2 Preparation of QDs conjugates via CDI, EDC, EDC/NHS

In this work, we used so called zero-length-cross-linking agents: CDI, EDC and EDC with addition of NHS, as coupling agents.

In order to produce BSA QDs conjugates, in first experiment we used CDI (10 mm^3, 10 mmol dm^{-3}) containing PBS buffer (100 mmol dm^{-3}, pH 7.4) and added to the solution of orange CdTe QDs (1000 mm^3, 1 mg dm^{-3}). The solution was incubated at room temperature for 30 min to activate carboxyl groups. Then, different concentration BSA (200 mm^3; 7.52 ×

10^{-8}, 1.50×10^{-7}, 3.00×10^{-7}, 4.51×10^{-7}, 6.00×10^{-7}, 7.52×10^{-7}, 1.31×10^{-6}, and 1.50×10^{-6} mol dm^{-3}) was added to the solution and incubated at room temperature for 2 h [35]. During the reaction of carboxyl groups on the surface of QDs with CDI, a reactive intermediate, N-acylimidazole, is formed with liberation of carbon dioxide and imidazole as innocuous side products. The N-acylimidazole can then react with amines form stable covalent amide or ester linkages, respectively (Figure 2) [33].

For producing BSA QDs conjugates in second experiment we used BSA (250 mm^3; 7.52×10^{-8}, 1.50×10^{-7}, 3.00×10^{-7}, 4.51×10^{-7}, 6.00×10^{-7}, 7.52×10^{-7}, 1.31×10^{-6}, and 1.50×10^{-6} mol dm^{-3}) and EDC (57 mm^3, 10 mg cm^{-3}) and added to the solution of orange CdTe QDs (250 mm^3, 0.1 mg cm^{-3}). The solution was then incubated at room temperature for 2 h [36]. 1-Ethyl-3-(3-dimethylaminopropyl)carbodiimide(EDC) reacts with a carboxyl group of QDs to form an amine-reactive O-acylisourea intermediate, which is highly unstable and short-lived in aqueous solution (Figure 2). Thus, hydrolysis is a major competing reaction [34].

It was found that the addition of sulfo-NHS stabilizes the amine-reactive intermediate by converting it to a semi-stable amine-reactive sulfo-NHS ester, thereby increasing the efficiency of EDC mediated coupling reactions (Figure 2) [15].

For producing another type of BSA QDs conjugates we added EDC (200 mm^3, 50 mmol dm^{-3}) and sulfo-NHS (200 mm^3, 5 mmol dm^{-3}) to the solution of orange CdTe QDs (200 mm^3, 0.1 mg cm^{-3}). The solution was incubated at 32 °C for 30 min. Then, BSA (200 mm^3; 7.52×10^{-8}, 1.50×10^{-7}, 3.00×10^{-7}, 4.51×10^{-7}, 6.00×10^{-7}, 7.52×10^{-7}, 1.31×10^{-6}, and 1.50×10^{-6} mol dm^{-3}) was added to the solution and incubated at 32 °C for 2 h while shaking [37].

For synthesis of QDs conjugated to antibody and antigen, method described in further text was used.

Mixture of EDC (200 µL, 50 mM) and sulfo-NHS (200 µL, 5 mM) were added to the solution of both orange and green CdTe QDs (200 µL, 0.1 mg mL^{-1}). The solution was incubated at 32 °C for 30 min. Then, different concentration of 200 µL anti-BSA, was added to the solution of green QDs and 200 µL with different concentration anti-IgG was added to orange QDs and incubated at 32 °C for 2 h while shaking. This conjugation procedure is simple, fast and selective to carboxyl groups on the QD surface and primary amino groups of a protein. After formation of QDs-antiBSA and QDs-antiIgG, BSA and mouse IgG were added while shaking at the room temperature. The resulting solution contained stable QDs-immunocomplex without obvious aggregates and was ready for assay.

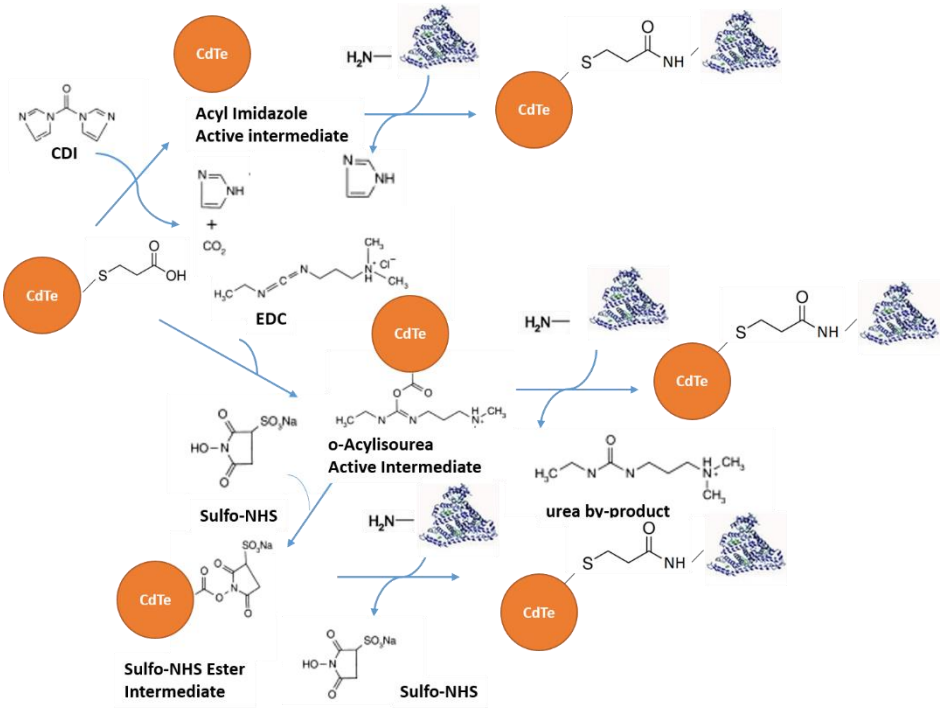

Figure 2 Bioconjugation reaction scheme of CdTe–MPA QDs to BSA

3.3 Equipment used for characterization of pure QDs and their conjugates

3.3.1 Measure of Fluorescence

Fluorimetric analysis was performed using multifunctional microplate reader Tecan Infinite 200 PRO (TECAN, Switzerland). 380 nm was used as an excitation wavelength and FL scan within the range from 420 to 800 nm was measured with 2 nm steps. Each intensity value is an average of five measurements. The detector gain was set to 60. 200 mm^3 of the sample (QD–BSA conjugates coupled via CDI, EDC or EDC/sulfo-NHS, CdTe–MPA QDs) was placed in transparent 96 well microplate with flat bottom by Nunc (Thermo Scientific, USA).

3.3.2 Dynamic light-scattering measurements

Dynamic light-scattering measurements were recorded on the DynaProNanoStar (WYATT Technology, USA). The measurements were performed at constant temperature (25 °C) in disposable plastic cuvette. Samples were filtered through a 0.22 mm membrane filter prior to measurements. The light source was an argon-ion laser (DynaPro NanoStar, Wyatt Instrument Technology, λ = 658 nm) and photons scattered by the sample were collected at angle 90°, multi-tau correlator was used for analysis of diffusion coefficients resulting in micelle size, and dynamics software was employed to results evaluation. d_{hydr} was calculated from the translational diffusion coefficient using Stokes–Einstein equation.

3.4 CE chip fabrication

To decrease the analysis cost as well as carryover effect, a single-use polymeric microfluidic chips were used in this study.

The easy and reliable production suitable for large-quantity preparation increased the reproducibility of the analyses due to the minimization of errors caused by lithographic procedure.

Rapid prototyping of a chip starts with creating design for a device in a computer/aided design software. A high-resolution printing is used to print design on a chrome transparency mask. This transparency serves as a photomask in photolithography to produce a positive relief of photoresist on silica wafer. Silica mold with channels of 50 µm width was made and used for rapid molding of PDMS.

3.4.1 Lithography

Photolithography was used to fabricate mold with microchannels. Next steps were performed to fabricate mold with channels (Figure 3) :

1. A blank 100 mm diameter Silicon wafer (Si (100) wafer, n-type, 500nm of SiO_2 layer) was rinsed with isopropyl alcohol, deionized water, and dried with N_2 gun. To increase adhesion of photoresist on the silicon wafer, surface was treated with Hexamethlyldisilazane (HDMS) for 5min.
2. AZ 1518 positive photoresist was spinned (2-step spinning parameters : step one- 500 rpm, 5sec; step two- 4000 rpm, 45sec) to create uniform film ~ 2µm thick. Wafer was pre-bake on a hot plate (100^{O}C for 2 min).
3. Wafer was exposed with 2500 mJ/cm^2 at 405 nm through a photomask. Post/bake was done at 200^{O}C for 1 min. Wafer was developed in AZ 327 for 40 sec, rinsed in isopropanol and dried with N_2 gun.
4. Etching of silicon dioxide, to remove areas of silicon dioxide unprotected by photoresist,

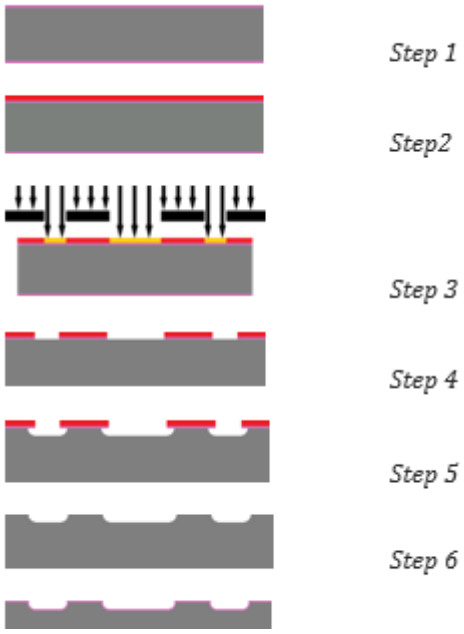

Figure 3 Lithography steps for fabrication of silica mold

was done using buffered oxide etch (BOE) solution (6 parts of 40% NH_4F and 1 part of 49% HF) for 20 sec.

5. XeF_2 was used for dry isotropic etching of silicon.

6. Rinsing with isopropyl alcohol was done to remove photoresist. Polishing of surface of wafer with microchannel was done using mixture of HNO_3 and BOE (buffered oxide etch) (100:1).

7. Wafer mold was cleaned using piranha solution (mixture of sulfuric acid (H_2SO_4 and hydrogen peroxide H_2O_2) for few seconds.

3.4.2 PDMS molding

A mixture of the PDMS prepolymer and curing agent at a ratio of 10:1 (w/w) was completely degassed and poured onto the silica mold, which was cured for 2 h at 65 °C, and peel off. After air drying of channels, PDMS is punched to make holes (2 mm) as fluid reservoirs. The patterned side of the PDMS was treated with oxygen plasma (200 W, 15 min) and bonded permanently with a plasma-treated glass substrate to form a closed fluidic system (Figure 4). The microfluidic chip contained fabricated channels ≈50 µm width and ≈5 µm depth. The chip design is shown in Figure 5.

./ 9999

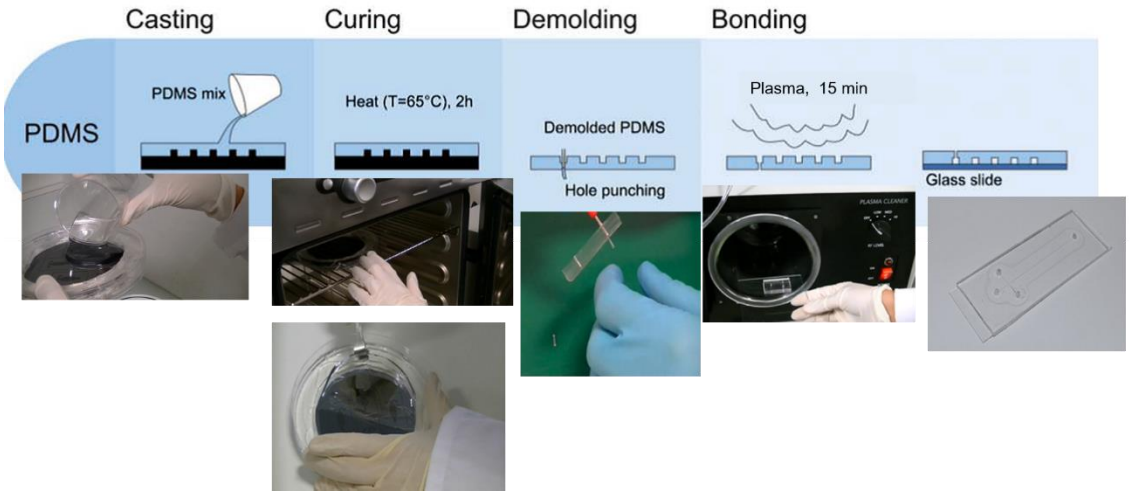

Figure 4 Creating of PDMS-glass microfluidic chip

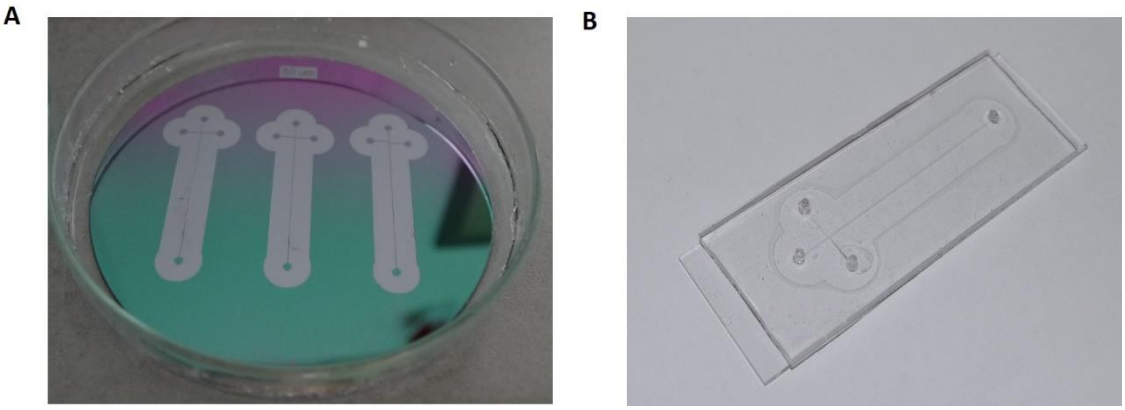

Figure 5 A) Fabricated mold with microchannel B) final look of fabricated chip

3.5 PDMS surface treatment

When using polymer care must be taken in control of surface chemistry. One of the main disadvantages of using PDMS channel, is that walls are not natively charged, and those cannot produce strong EOF, which is necessary to move analytes toward detector as well as to electro-kinetically manipulate fluid flow [38]. Low thermal conductivity of PDMS can lead to rise in temperature due to resistive heating in electrophoresis. This rise in temperature causes broadening of peaks and lowers the resolution of system. Also adsorption of hydrophobic analytes into native PDMS, has been reported [39]. To overcome this problem modification of PDMS is necessary. Surface of PMDS can be either dynamically or permanently modified. Dynamic coatings such as SDS, or TTAB [40], oxidation with plasma[41] and covalent modification [42].

In our work the patterned PDMS side was exposed to oxygen plasma for 15 minutes and surfactant Tween 20 was added to a running buffer.

Results of separation of CdTe QDs conjugated with BSA, using on a chip CE, before and after PDMS surface treatment was shown in Figure 6. Clearly it can be noticed that no surface treatment results in broad peak and poor separation resolution.

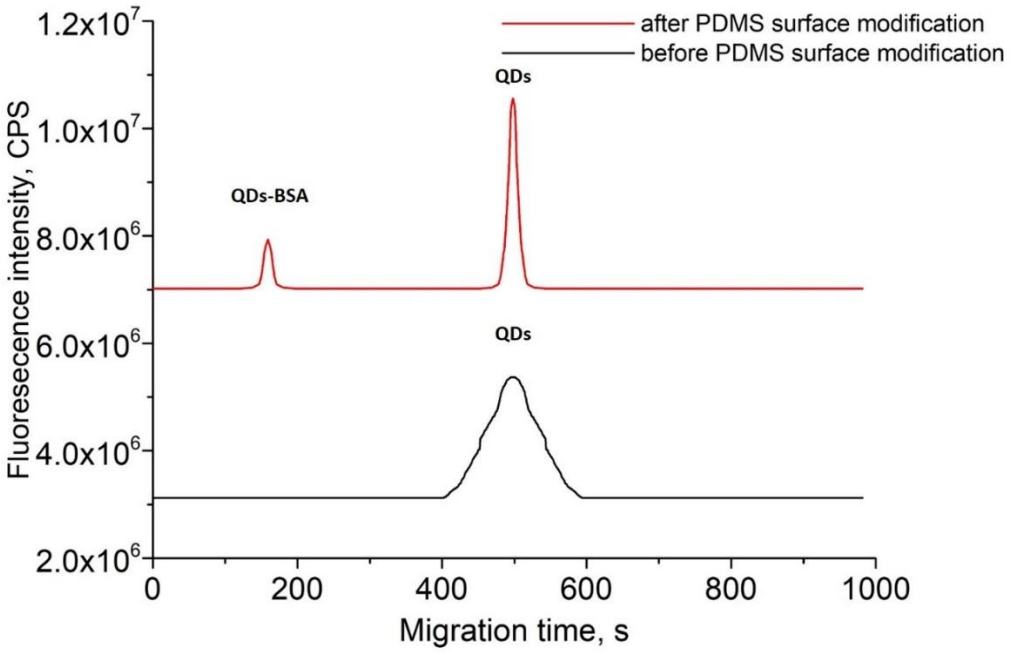

Figure 6 Electropherograms of separation of the QDs and bioconjugated QDs with BSA, before and after surface plasma modification of PDMS chip

Exposing PDMS replica to plasma introduces polar groups on the surface. Plasma introduce silanol groups (Si-OH) at the expense of methyl groups (Si-CH_3) [43]. This silanol groups condense with appropriate groups (OH, COOH, ketone…) on another surface, when they are brought together. In PDMS-glass contact these are SiO-Si bonds. These covalent bonds make tight, irreversible seal. As already mentioned PDMS has hydrophobic surface. This surface is hard to wet with other aqueous solutions, and making adsorption of other hydrophobic species as well as nucleate bubbles. Exposure to plasma makes surface more hydrophilic due to presence of silanol groups. Due to this aqueous solution can easily wet surface of channel, this also makes on the walls of channel ioniziable groups ($SiOH \leftrightarrow SiO^- + H^+$). These groups will in contact of basic and neutral solutions support strong EOF toward cathode. Nevertheless, this negatively charged channels have great resistance to adsorption of hydrophobic and negatively charged analytes. When using this process care must be taken in choice of a gas, timing after plasma, and cleanliness.

When using PDMS chip for separation of bioconjugated QDs adsorption of biomolecule was observed which was resulting in broad peak and poor separation resolution. To overcome this problem in our work surfactant Tween 20 was used. Surfactant is added into the running buffer to achieve the hydrophilic PDMS surface. The hydrophobic tails of the amphiphilic surfactant molecules were adsorbed onto the PDMS surface while the hydrophilic heads stick out in the buffer, thereby changing the PDMS surface properties. In this way, surface modification can be accomplished faster, cheaper and simpler [44] .

3.6 Instrumental set up and data acquisition

On a chip electrophoresis were carried out using a developed electro-optical system. The system consists of the five parts: light source, sample holder, light detector, control electronics and high voltage generator. Excitation light is generated by ultraviolet light-emitting diode (UV LEDs Roithner Laser Technik GmbH, λmax = 375 nm, output power 5.5 mW) and filtered by optical 380 nm low-pass filter (BAADER U-Filter No.: 2458292). This light excites FL of the sample and emitted light is selected by 420–680 nm high-pass optical filter (BAADER UV/IR-Cut/L filter No.: 2459207A) and https://www.edmundoptics.com/p/520nm-cwl-10nm-fwhm-125mm-mounted-diameter/20157/. This emitted light is detected by photodetector including photomultiplier (Perkin Elmer, MP 963, spectral response 185–850 nm).The system is powered from low voltage source Agilent and sample flow control is provided by linear syringe pump. The applied voltage for the electrophoretic separation was ≈3 kV. This high voltage was generated from 5V voltage source.

The prepared microfluidic chips were connected to the small laboratory-made electrophoretic system employing light emitting diode as a miniaturized, low-energy consuming and low-cost excitation source. The system was equipped with a special optical filter holder enabling simple filter replacement and miniaturized photomultiplier tube for signal detection. Optical part with chip were placed into black box to avoid room light interference and insensitivity to temperature changes. The photograph of the instrumental set up as well as the scheme of connection of all necessary components are shown in Figure 7.

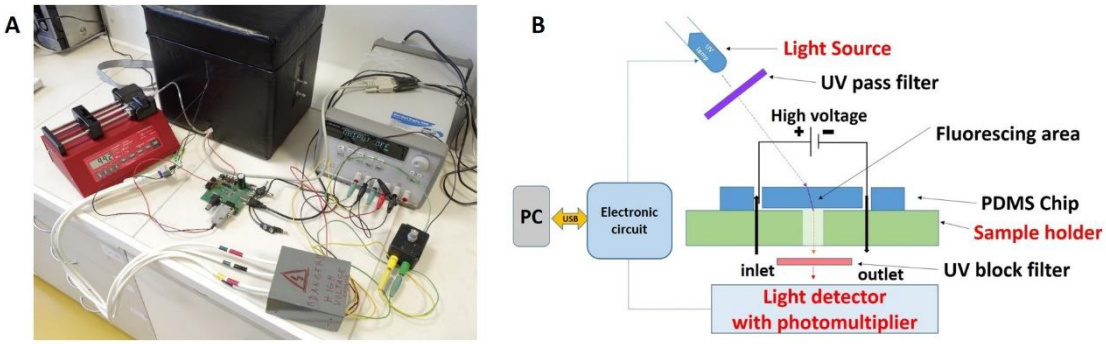

Figure 7 A) Photograph of the experimental setup, syringe pump, and power supply. B) Scheme of the electro-optical system

3.6.1 CE procedure

The fabricated chip is placed on the sample holder (Figure 8) and microchannels are first filled with buffer. 100 µL of sample, prepared as mentioned above, was loaded in inlet reservoir. After filing the sample reservoir, platinum electrodes are placed in each fluid reservoir and contacted to power supplies. CE separation was accomplished with an effective length of ≈8 cm between inlet and detector (total chip length ≈10 cm). Initially a new chip was flushed with 0.1 mL NaOH (10 min), water (10 min), and running buffer (10 min). 10 mL Borate buffered saline buffer (BBS, pH ≈9.14) was used as a BGE. The mobility of the EOF, which transported analytes from the injection reservoir to the detector at the negative voltage, was determined using coumarin as a neutral marker. All solutions were filtrated through a 0.45 µm membrane filter before use. The read out from electronics was sent to laptop, and application enabling to save data in excel file was used.

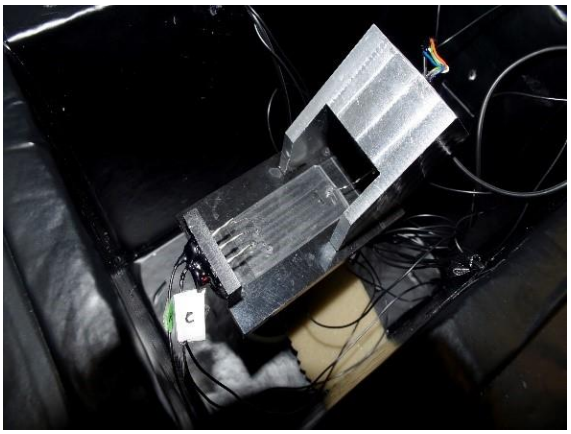

Figure 8 The prepared microfluidic chips connected to the laboratory-made electrophoretic system

3.7 Characterization of QDs and their conjugates

3.7.1 MPA coated QDs characterization

Water-soluble CdTe QDs were synthesized and stabilized with 3-mercaptopropionic acid (MPA). QDs used in this study showed narrow and symmetrical emission spectrum excited at 380 nm on multimode microplate Tecan reader. It was found that FL intensity is increasing with increasing of reaction time and the red shift was observed. QDs exhibit a strong emission of red light with emission maximum at 600 and 76 nm of full-width at half-maximum (FWHM) after 4 h of reaction (Figure 9). The sample with reaction time of 4 h showed the highest FL and was chosen for further conjugation with protein. The absolute quantum yield of QDs was evaluated to be 16.5% by Quanta u quantum yield measurement

system (FluoroLog, HORIBA Jobin–Yvon). The ‘‘blank experiments’’ using bioconjugation agents (CDI, EDC, and sulfo-NHS) and BSA were done to be sure that there is no contribution of side products to luminescence of system (Figure 9).

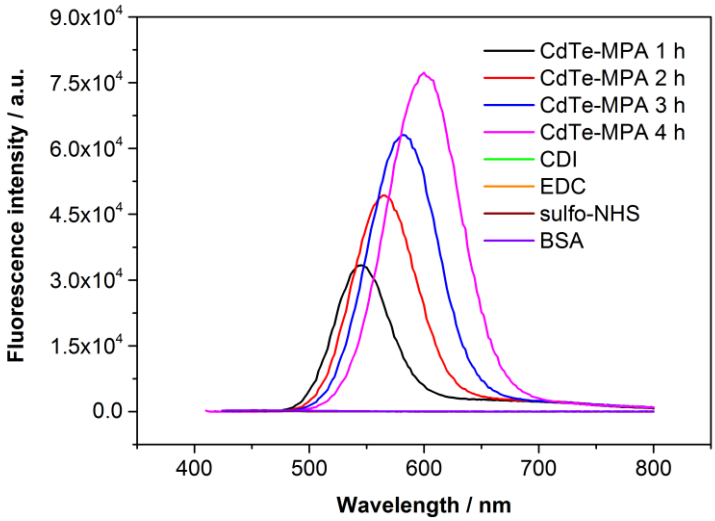

Figure 9 Emission spectra of MPA-capped CdTe QDs at different reaction times: 1, 2, 3, and 4 h; pure CDI, EDC, sulfo-NHS and BSA, and excitation wavelength at 380 nm

The crystal structure of CdTe QDs was examined with powder X-ray diffraction (XRD) on Empyrean X-ray diffractometer, PANalytical. The XRD pattern of CdTe QDs shows diffraction peaks at positions $2\Theta \approx 24^0$, 40^0, and 46^0 which are indexed corresponding to prominent orientation (111) and two other weak orientations (220) and (311), respectively (Figure 10). These confirm that synthesized CdTe is in cubic zinc blende structure and lattice is face-centered system. The intensity of XRD peak indicates that synthesized CdTe QDs are crystalline and broad diffraction peaks indicate very small-sized crystals [45].

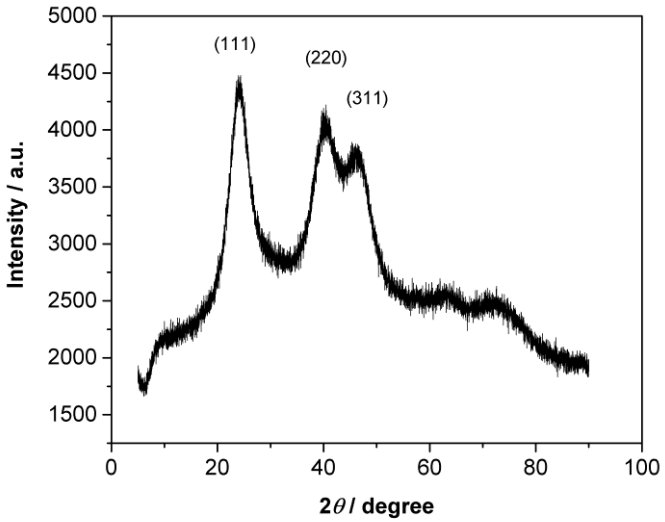

Figure 10 X-ray diffractogram of powder pattern of MPA-capped CdTe QDs

Dynamic light-scattering (DLS) measurements were performed to determine the hydrodynamic radius of QDs before and after conjugation with protein. The hydrodynamic diameter (d_{hydr}) of CdTe–MPA QDs was found to be (2.8 ± 0.5) nm and represents mean value ± standard deviation and three measurements. There is a significant increase in diameter size after conjugation. This confirms the successful conjugation of a protein on a surface of QDs. When using EDC/sulfo-NHS as a cross-linker and after BSA coating, d*hydr* was determined as (7.1 ± 0.1) nm (mean value ± standard deviation, 3 measurements) which perfectly correlates with the literature [28]. MPA- and protein-conjugated CdTe QDs are well dispersed in phosphate-buffered saline (PBS) buffer, and there were no agglomerates or formed clusters of several QDs. Table 1 summarizes the data from DLS measurements.

Table 1 Hydrodynamic diameters of CdTe–MPA QDs before and after bioconjugation with BSA using different cross-linkers, determined by DLS

Type of cross-linker	d_{hydr}/nm (mean value ± standard deviation)	
	CdTe-MPA	CdTe-MPA-BSA
CDI	2.8 ± 0.5	5.5 ±0.1
EDC		5.8 ±0.1
EDC/sulfo-NHS		7.1 ±0.1

3.7.2 Conjugated QDs characterization

In this work, so called zero-length-cross-linking agents were used as coupling agents. Two step procedure combining EDC with sulfo-NHS that conjugates carboxyl and amine groups to form stable covalent amide linkages was used.

The optical properties of QDs are strongly dependent on their size which can be easily controlled by the time of synthesis. Therefore, two types of CdTe QDs differing only in the size were conjugated with two different antibodies. The optical characteristics of the bioconjugated QDs are shown in Figure 11. Narrow and symmetrical emission spectra were observed when excited by 350 nm. It clearly follows from these results that the emission maximum of the anti-BSA-modified CdTe QDs is at 532 nm (green emission), while the emission maximum of the anti-IgG-modified CdTe QDs is at 610 nm (orange emission). The photograph of the solutions of bioconjugated QDs under UV light illumination is shown in the inset in Figure 11A

Bioconjugation reaction scheme of CdTe–MPA QDs to anti-BSA and anti-IgG via covalent coupling is shown in Figure 11C. First, CdTe–MPA QDs were prepared in aqueous solution phase. The thiol group of MPA is linked to the surface of CdTe QDs by thiol group-Cd coordination, and the functional carboxylic group is free, which can be easily coupled to biomolecules with amino groups, such as proteins, peptides, and amino acids. So-called zero-length-cross-linking agents and two-step procedure combining EDC with N-hydroxysulfosuccinimide (sulfo-NHS) was used as a coupling agent, that conjugate carboxyl groups and amines to form stable covalent amide linkages.

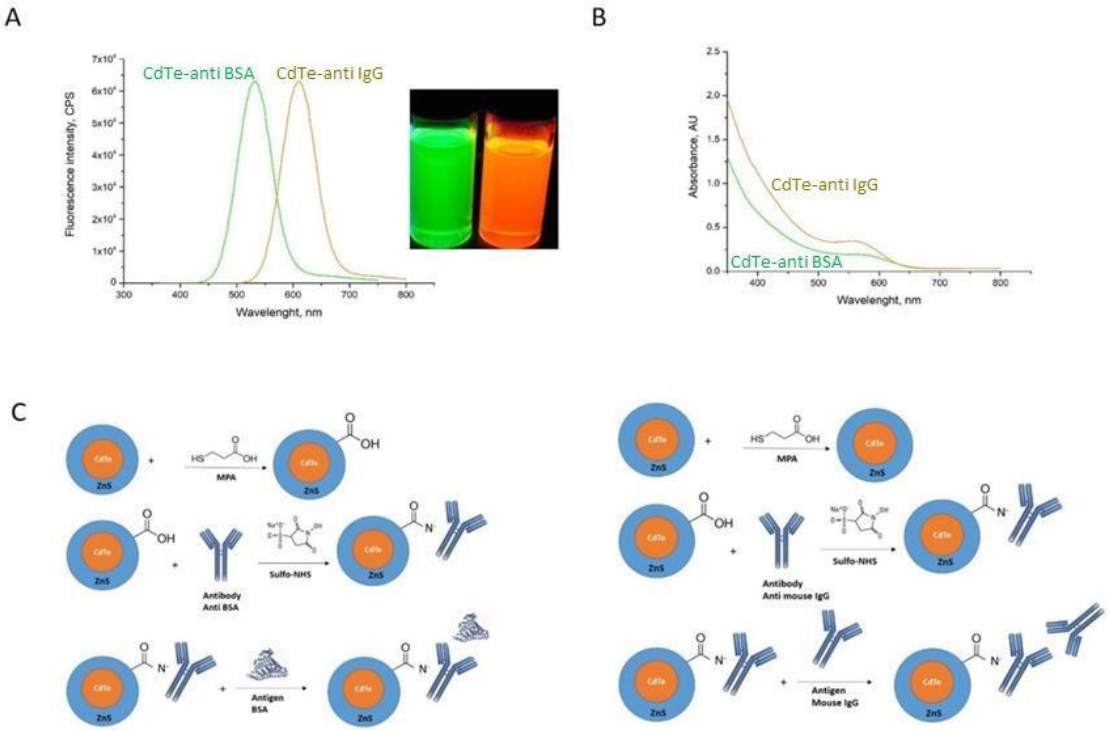

Figure 11 Characterization of quantum dots. A) emission spectra of bioconjugated QDs inset: photograph of QDs solution under UV light illumination, B) absorption spectra of bioconjugated QDs, C) Bioconjugation reaction scheme of CdTe–MPA QDs to anti-BSA (left) and anti-IgG (right)

4 STUDYING OF QUANTUM DOT LUMINESCENCE QUENCHING EFFECT CAUSED BY COVALENT CONJUGATION WITH PROTEIN

4.1 On-a-chip electrophoresis of bioconjugated QDs

Binding of QDs with biomolecules can be determined by measuring the changes in the electrophoretic mobility overtime of bioconjugated QDs by CE, since interaction with these molecules will result in changes in the hydrodynamic size of QDs [46]. First, CdTe–MPA QDs were prepared in aqueous solution phase. The thiol group of MPA is linked to the surface of CdTe QDs by thiol group-Cd coordination, and the functional carboxylic group is free, which can be easily coupled to biomolecules with amino groups, such as proteins, peptides, and amino acids. Coupling agent CDI, EDC, and EDC/sulfo-NHS were used to bioconjugate QDs with BSA. We studied the most suitable coupling agent for BSA conjugation with QDs. The CE was used for separation QD–BSA complex and unbounded QDs in the sample solution.

Figure 12 shows biomolecule conjugate electrophoretic behavior. The free QDs are well separated from QD–BSA within 10 min in the alkaline buffer (10 mM BBS). The migration times of conjugates were determined in comparison with non-conjugated QDs based upon their charge to-size ratio values. The QD–BSA conjugates were detected at a shorter migration time (2 min 40 s) compering free QDs (9 min 20 s) due to the inherent increase in the net negative charge of the conjugate. The isoelectric point (pI) of BSA is lower than CE buffer pH and thus increased number of negative charges that also influenced the net charge of the conjugate [32].

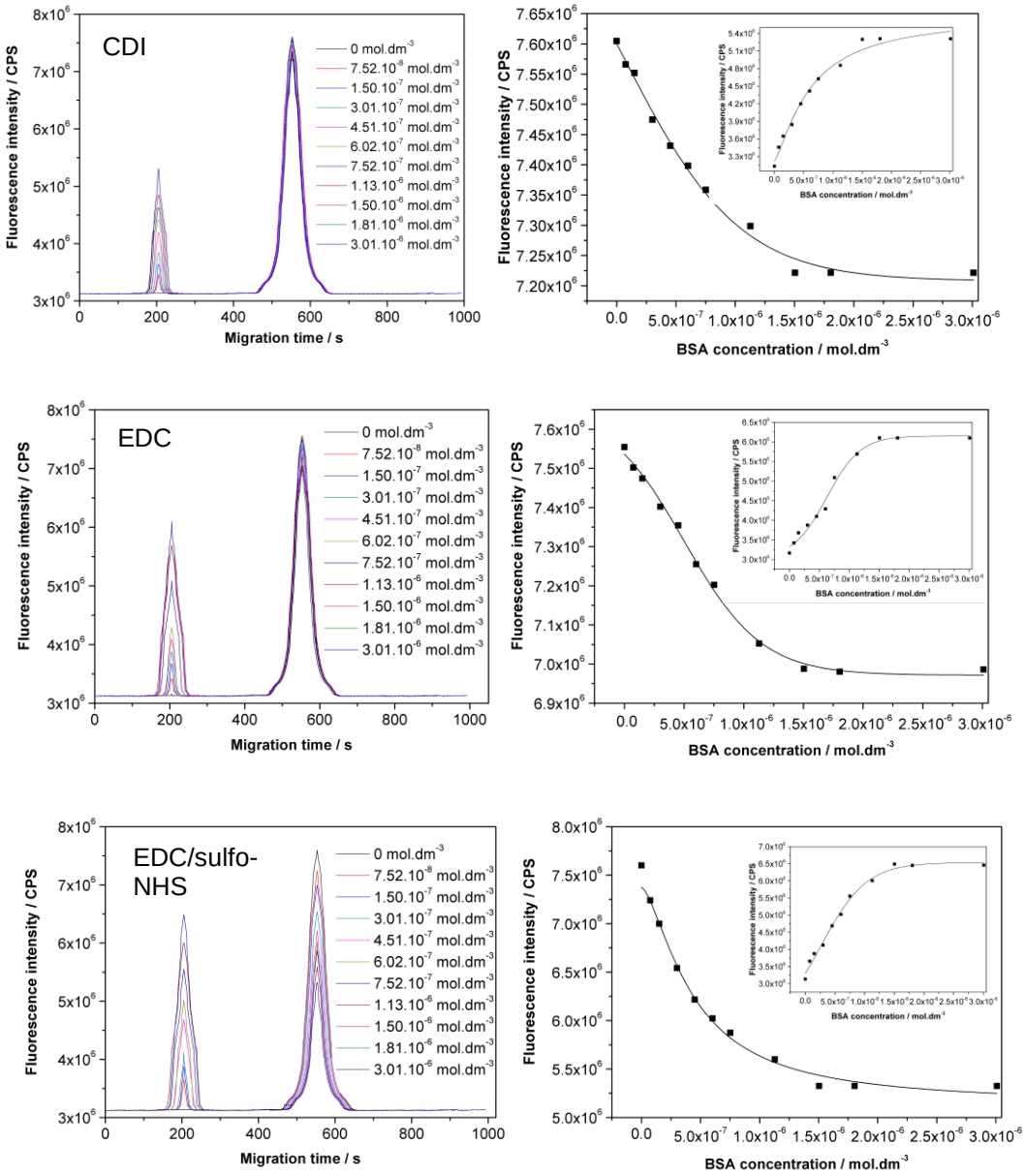

Figure 12 Electropherogram for separation of the CdTe-MPA QDs bioconjugated with various concentration of BSA, using different coupling agents, CDI, EDC and EDC/sulfo-NHS (left). Trend of QDs peak decreasing with increasing of BSA concentration was also shown (right). Inset: Trend of QDs-BSA peak increasing with increasing of BSA concentration. On a chip CE conditions- excitation: 380 nm; emission: 600 nm; channel: 50 µm, 10/4 cm; BGE: 10 mM Borate Buffered Saline (BBS), pH 9.4; voltage: 3 kV; electroosmotic flow (EOF) mobility $44.4 \cdot 10^{-9}$ $m^2 \cdot V^{-1} \cdot s^{-1}$.

The influence of increasing protein concentration on FL was studied. FL of free QDs (QDs peak) is decreasing and FL of QDs bioconjugates (QD–BSA peak) is increasing with increasing of protein concentration. In case of using CDI as a cross-linker, according to the plots (Figure 12, CDI right) at lower concentration of protein (in the range from 7.52 x 10^{-8}

to 1.50 x 10^{-6} mol dm-3), QD peak intensity decreased for 5% (from 7.60 x 10^6 CPS to 7.22 9 10^6 CPS) and QD– BSA peak intensity increased for 37% (from 3.13 x 10^6 CPS to 5.29 x 10^6 CPS) with a linear trend (Figure 12, CDI right inset). At higher concentration (>1.50 x 10^{-6} mol dm^{-3}) of protein, plateau on the dependence curve is noticed.

In case of using EDC as a cross-linker according to the plots (Figure 12, EDC right), at lower concentration of protein (in the range from 7.52 x 10^{-8} to 1.50 x 10^{-6} mol dm^{-3}), QD peak intensity decreased for 7.6% (from 7.55 x 10^6 CPS to 6.98 x 10^6 CPS) and QD–BSA peak intensity increased for 47% (from 3.16 x 10^6 CPS to 6.01 x 10^6 CPS) with a linear trend (Figure 12, EDC right inset). At higher concentration (>1.50 9 10^{-6} mol dm^{-3}) of protein, plateau on the dependence curve is noticed. It was found that the addition of sulfo-NHS stabilizes the amine-reactive intermediate by converting it to a semi-stable amine-reactive sulfo-NHS ester, thereby increasing the efficiency of EDC mediated coupling reactions (Figure 2)[15].

In case of using EDC/sulfo-NHS as a cross-linker, according to the plots (Figure 12, EDC/sulfo-NHS right) at lower concentration (in the range from 7.52 x 10^{-8} to 7.25 x 10^{-7} mol dm^{-3}), QD peak intensity decreased for 30% (from 7.60 x 10^6 CPS to 5.32 x 10^6 CPS) and QD–BSA peak intensity increased for 52% (from 3.13 x 10^6 CPS to 6.48 x 10^6 CPS) with a linear trend (Figure 12, EDC/sulfo-NHS right inset). At higher concentration (< 1.13 x 10^{-6} mol dm^{-3}) of protein, plateau on the dependence curve is noticed. The most rapid decreasing and increasing of peaks intensity was noticed when using EDC/sulfo-NHS, compared to EDC and CDI. Plateau of peak shows a saturation of BSA ligands on a QD surface, and it occurs at 1.50 x 10^{-6} mol dm^{-3} concentration of protein for CDI and EDC and at lower concentration of protein 7.25 x 10^{-7} mol dm^{-3} for EDC/sulfo-NHS cross-linker. The sulfo-NHS ester is more effective at reacting with amine-containing molecules. When using this two-step process as opposed to using single-step EDC or CDI reaction, higher yields of amide bond formation may be achieved, which lead to saturation of BSA on QD surface at lower concentration.

4.2 Studying of fluorescence quenching of QDs caused by covalent conjugation with BSA

Quantum dots and BSA were conjugated via covalent coupling using three different agents CDI, EDC, and EDC/sulfo-NHS. FL intensity of bioconjugated QDs was measured by Tecan reader and it is decreasing with increasing of concentration of BSA. For further study of QD FL quenching, we processed different concentrations of protein up to 1.50 9 10-6 mol dm-3, where quenching effect is significant. Fluorescence-quenching effect of QDs caused by BSA can be described by the linear Stern–Volmer equation (1) [36].

$$\frac{I_0}{I} = 1 + K_{sv}\,[Q] \qquad (1)$$

Where I_0 and I are steady-state FL intensities of QDs in the absence and presence of BSA, respectively, K_{SV} is the Stern-Volmer quenching constant, and [Q] is the concentration of BSA. The I_0/I were calculated according to (1) and plotted against BSA concentration (Figure 13).

The dependences exhibited very good linearity with coefficients of determination R^2 in the range of 0.97–0.98 for all three coupling agents— CDI, EDC, and EDC/sulfoNHS. After linear fit, the slopes of the curves were calculated. The values represent K_{SV} and the higher K_{SV}, the higher the quenching effect is [47]. The results show that the quenching constants vary for different types of bioconjugated QDs and depend on type of coupling agents used CDI, EDC, or EDC/sulfo-HNS and they are 3.64 x 10^4, 5.59 x 10^4,and 4.38 x 10^5 dm^3 mol^{-1},respectively,which is correspondent with values stated by other authors [48]. The Stern–Volmer plot of QD-quenching properties exhibited linear trend for the concentration given. This behavior suggests that only static quenching is taking place [49]. The results present that BSA can effectively quench FL of QDs in a ligand-dependent manner. In case where EDC/sulfo-NHS is used as a cross-linker, the FL is decreasing significantly, so the highest quenching effect was notable (see Figure 13).

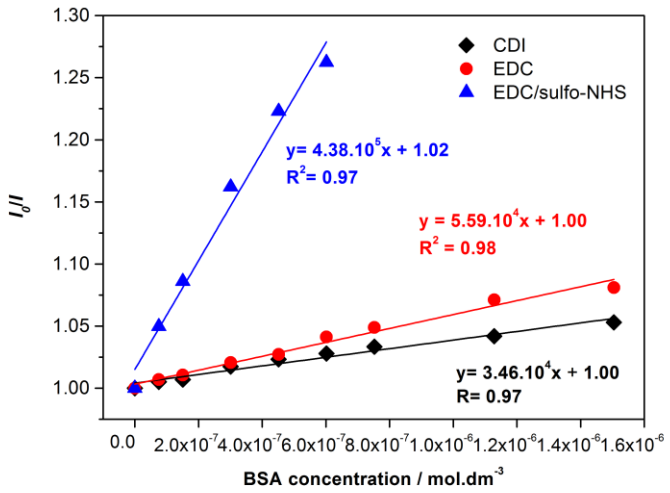

Figure 13 Stern–Volmer plots of BSA concentration dependence of FL intensity of QDs. I_0 and $I$are FL intensities of QDs in the absence and presence of BSA, respectively. Effect of cross-linker on a QD–BSA interaction was shown

The occurrence of static-quenching mechanism enlightened the presence of binding sites in the BSA. The binding sites and binding constant can be calculated from the following Equation (2) [48]:

$$\log\left[\frac{(I_0-I)}{I}\right] = \log K + n \cdot \log[\mathrm{Q}] \qquad (2)$$

where K is the binding constant and n is number of binding sites between BSA and QDs. Based on (2) log [(I0-I)/I] were plotted against log[Q] for all three cross-linkers (Figure 14). The values of n (slope values) and K (intercept values) were calculated from the plots.

The results show that the binding constants vary for different types of bioconjugated QDs and depend on type of coupling agents used CDI, EDC, or EDC/sulfo-NHS and they are 3.16×10^3, 9.18×10^3, and 2.24×10^4 dm^3 mol^{-1}, respectively. Values of binding constants calculated from this approach show similar trend as K_{SV} calculated from the Stern–Volmer equation. The highest binding constant was determined for QDs coupled with BSA using EDC/sulfo-NHS. These results again confirm that the quenching mechanism is the static (complex formation) [48]. The number of binding sites is close to 1 for different ligands of QDs, suggesting that there is only one type of interaction between BSA and QDs [50].

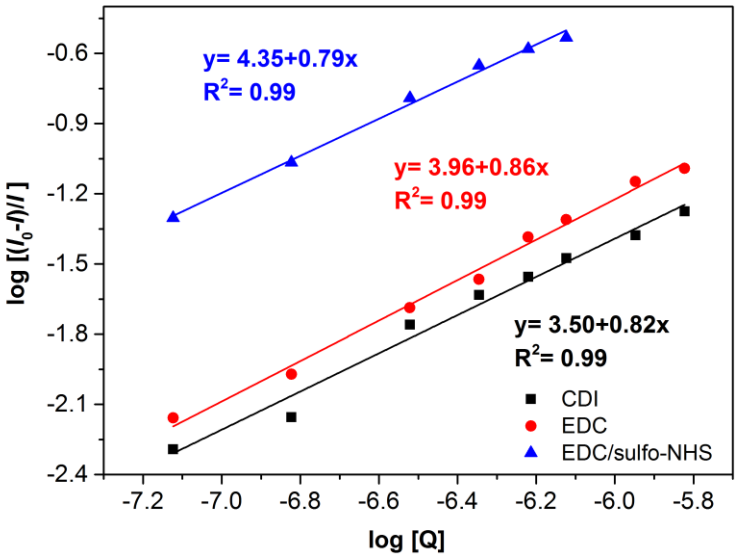

Figure 14 Plots of log [(I_0–I)/I] versus log[Q] for different cross-linkers. I_0 and I are FL intensities of QDs in the absence and presence of BSA, respectively

The presence of BSA protein leads to strong quenching of FL emission, which could be explained by covalent interaction between the QDs and the quencher, demonstrating the formation of QD–BSA bioconjugates [40]. The sulfo-NHS ester is increasing the efficiency of coupling reactions; thus, the highest binding constant and quenching constant were determined when using EDC/sulfo-NHS as a cross-linker. The relative standard deviations of the migration time and peak area for QD–BSA with six runs were ≈2.1 and ≈8.7%, respectively.

5 ON A CHIP ELECTROPHORESIS IMMUNOASSAY FOR MULTIPLE ANTIBODIES

5.1 Electrophoretic analyses of antigen-antibody reaction products

The optimized system for efficient QD immunoassay based on a separation method should provide a clear resolution of three zones; the zone of unreacted QDs, free conjugates of QD with an antibody and the immunocomplex [19]. Such separation is demonstrated in Figure 15.

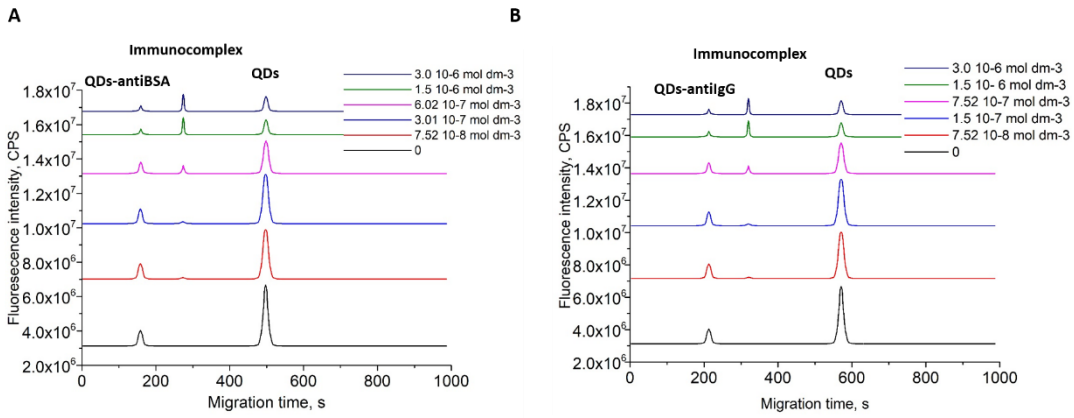

Figure 15 Electropherograms of separation of the Ab-QDs immunocomplexes with various concentrations of antigen. A) green QDs with BSA, B) Orange QDs with IgG

To evaluate analytic performance of the proposed strategy, the fluorescence intensity was measured in the presence of antigen at different concentrations. At lower concentrations of BSA (in the range from 0.005-0.1 mg/ml), QDs–Ab peak intensity decreased with a linear trend (Figure 16 A), while immunocomplex peak increased also with

a linear trend. At higher concentration of BSA (<0.1 mg/ml), a plateau on the dependence curve is noticed.

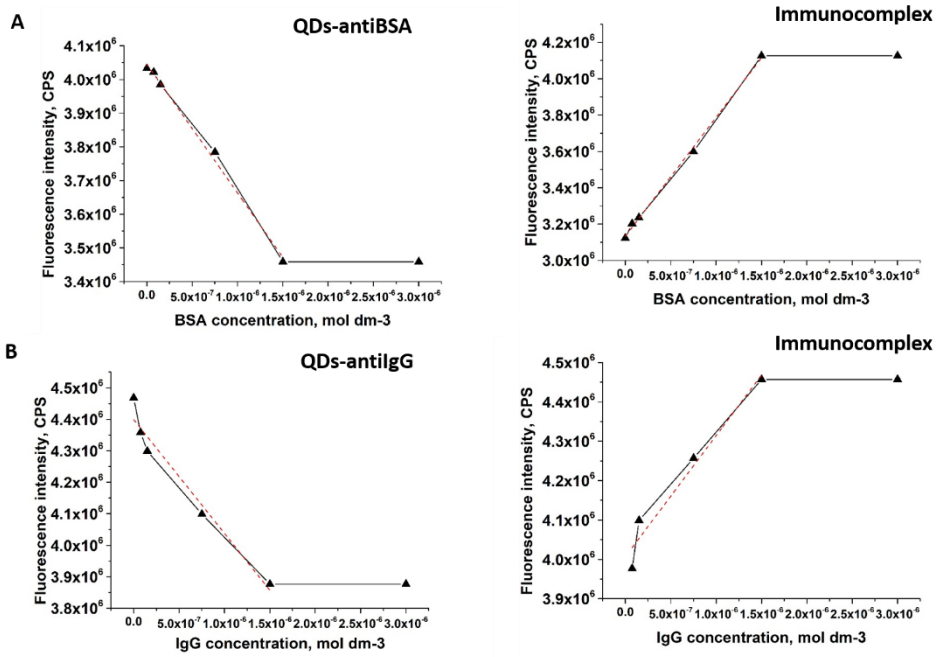

Figure 16 Dependence of QDs- antibody and immunocomplex peaks height on antigen concentration. A: Green QDs with BSA as an antigen, B: Orange QDs with IgG as an antigen

In case when IgG was used, same dependences for peaks are noticed. At the concentration of IgG in the range from 0.005-0.1 mg/ml, peak intensity of QDs–Ab peak intensity decreased with a linear trend (Figure 16 B), while immunocomplex peak increased also with a linear trend. At concentration of IgG above <0.1 mg/ml, plateau on the dependence curve is noticed again for all three peaks.

Reached plateau translates in a saturation of immunocomplex on a QD surface, and it occurs at 0.1 mg/mL concentration of antigen for both BSA and IgG. The decrease in QDs-Ab and increase in QDs immunocomplex peak height or area is proportional to the amount of BSA and IgG present. The linear curve fitted equation and coefficient of determination represented are listed in Table 2.

Table 2 The linear curve fitted equation and their coefficient of determination

Sample	**Coefficient of determination,R^2**	**Regression equation**
Green QDs-BSA	0.9956	$y = -5.7 \times 10^6 x + 4.1 \times 10^6$
Orange QDs-IgG	0.9622	$y = -5.4 \times 10^6 x + 4.4 \times 10^6$
Green QDs- immunocomplex	0.9981	$y = 9.8 \times 10^6 x + 3.1 \times 10^6$
Orange QDs- immunocomplex	0.9566	$y = 8.6 \times 10^6 x + 3.7 \times 10^6$

5.2 Comparison of CE immunoassay and solid-phase immunoassay techniques

Compared to conventional immunoassays, CE immunoassays offer several possible advantages. Two important advantages of CE immunoassays are their ease of automation and their relatively fast separation of antibodies, analytes and/or antibody-analyte complex [51]. In addition, CE immunoassays tend to consume only small amounts of sample and reagents while still allowing the detection of trace amounts of analyte in a sample[52]. The detection of multiple analytes in a single run is also feasible in a CE immunoassay, due to the high resolving power of modern capillary electrophoresis system [53]. Unfortunately, CE immunoassays tend to give poorer concentration-based limits of detection than solid-phase immunoassay techniques such as an enzyme-linked immunosorbent assay (ELISA) [54] .

Under these experimental conditions, limit of detection (LOD) of the immunocomplex was estimated to be 9.1 μg/mL for BSA detection and 5.4 μg/mL for mIgG. This LOD values are relatively higher than that obtained by conventional ELISA (ng/mL-pg/mL order). CE immunoassays tend to give poorer concentration-based LODs than solid-phase immunoassay technique such as ELISA [54]. This is a result of the analytes and antibodies both being present in solution in many CE immunoassay formats, while in ELISA a surface reaction can be used to pre-concentrate analytes for measurement and detection. Consequently, these results suggest that the proposed device would enable simple and rapid immunoassays with minimal amounts of samples and reagents.

These facts make difficult to apply our proposed device for immunoassays of extremely low-concentration targets such as tumor markers for cancer. On the other hand, for the analysis of high-concentration intravital samples such as human IgG (ca. 7-16 mg/mL), the proposed device would enable us to easily measure analytes with a shorter analysis time, in comparison to conventional ELISA methods. Consequently, these results suggest that the proposed device would enable simple and rapid immunoassays with minimal amounts of samples and reagents.

5.3 Electrophoretic separation of the antigen-antibody-QD complex (immunocomplex) from the free antigen and influence of QDs concentration

Influence of pure QDs peak area on a concentration of antigen was studied. Under these optimal experimental conditions, we noticed gradually decreasing of pure QDs peak, with the increase of antigen antibody concentration. Final concentration of QDs was 0.1 mg/ml (Figure 17).

At lower concentration of BSA (in the range from 0.005-0.1 mg/ml), pure QDs peak intensity decreased for 40.2% with a linear trend (Figure 17). At higher concentration of BSA (<0.1 mg/ml), plateau on the dependence curve is noticed (Figure 17, right inset).

In case when IgG was used, same dependence for peaks is noticed. At the concentration of IgG in the range from 0.005-0.1 mg/ml, pure QDs peak intensity decreased for 40.7% with a linear trend (Figure 17, B right inset). At concentration of IgG above <0.1 mg/ml, plateau on the dependence curve is noticed

The decrease in QDs and QDs-Ab and increase in QDs immunocomplex peak height or area is proportional to the amount of BSA and IgG present. The linear curve fitted equation and coefficient of determination represented are listed in Table 3.

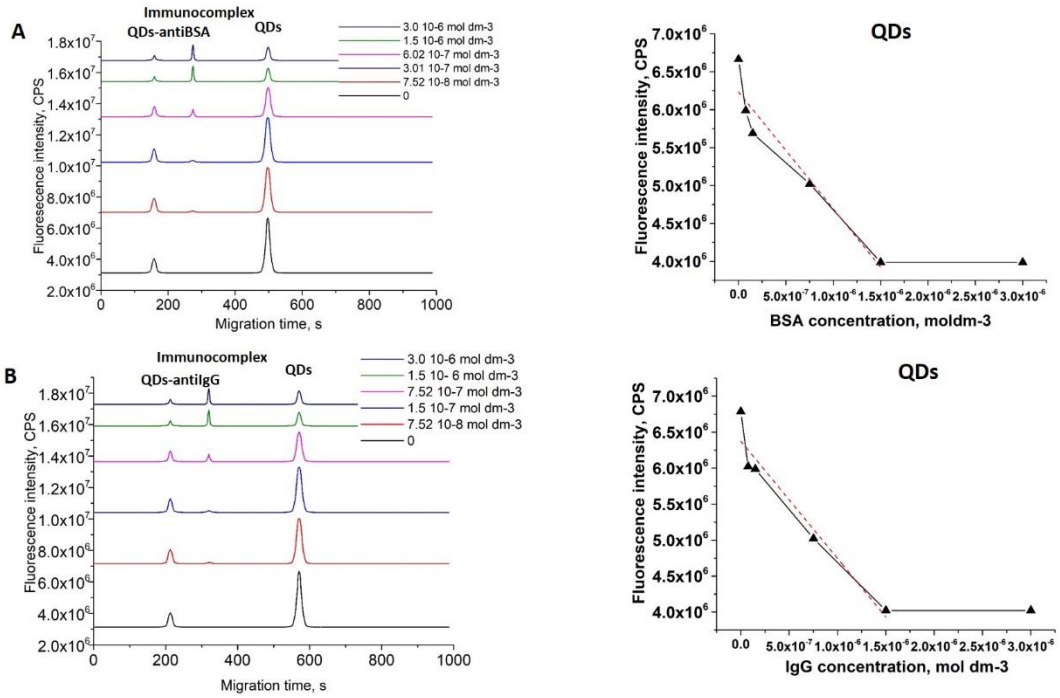

Figure 17 Electropherograms of separation of the Ab-QDs immunocomplexes with various concentrations of antigen. A) green QDs with BSA, B) Orange QDs with IgG (left). Dependence of QDs peak height on antigen concentration (right).

Table 3 The linear curve fitted equation and their coefficient of determination for pure QDs peak

Sample	**Coefficient of determination,R^2**	**Regression equation**
Free green QDs	0.9255	$y = -2.3 \times 10^7 x + 6.2 \times 10^6$
Free orange QDs	0.9411	$y = -2.4 \times 10^7 x + 6.4 \times 10^6$

Electrophoretic behavior of QD-biomolecule conjugate is shown in Figure 18. The free QDs are well separated from QDs- Ab and immunocomplex within 10 min in the alkaline buffer (10 mM BBS). The migration times of conjugates were determined in comparison with non-conjugated QDs based upon their charge to-size ratio values. Green QDs (1.8 nm ± 0.4) migrated faster towards detector than orange QDs (3.9 nm ± 0.7) due their smaller charge density. We were able to detect two different antigens simultaneously due its different size and charge. BSA as smaller protein migrated faster than IgG. The QD–BSA conjugates were detected at a shorter migration time (2 min 36 s) comparing to immunocomplex (4 min 31 s) and free green QDs (8 min 15 s). The QD-IgG conjugates were also detected at a shorter migration time (3 min 30 s) comparing to immunocomplex (5 min 17 s) and free orange QDs (9 min 28 s). Shorter migration time of conjugates and complex compare to free QDs occurs due to the inherent increase in the net negative charge of the conjugate. The isoelectric point (pI) of BSA (4.7) and IgG (7.0) is lower than CE buffer pH (8.2) and thus increased number of negative charges that also influenced the net charge of the conjugate [55].

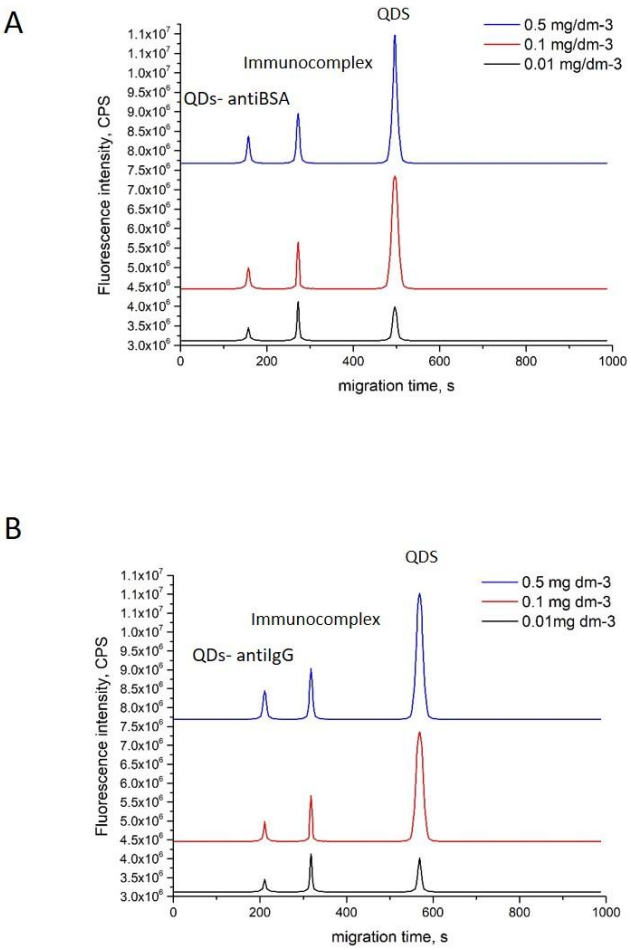

Figure 18 A: Electropherogram for separation of the CdTe–MPA QDs bioconjugated with A: green QDs with BSA, B: orange QDs with IgG, using different concentration of QDs (0.5, 0.1 and 0.01 mg/dm-3)

Figure 18 shows the complete separation of the conjugate and narrow peak of immunocomplex. It has already been described in literature that immunocomplex peak is much narrower than that of the QD-Ab conjugate [10]. This can be regarded as the evidence that only a limited number of the antibody molecules conjugated with QDs form a complex with the antigen. Thus, we can expect that the antibody conjugates capable of forming the immunocomplex are more homogeneous than those in the rest of the probe. Antibodies are complex structures with variable regions. The variation in the number of sialic acids attached to the heavy chain (Fc region) of an antibody causes the heterogeneity not only in its size but also in pI value. Another contribution to the polydispersity of a probe can be non-specific binding of the QDs at any primary amine group of a large antibody molecule. The antigen-binding sites of an antibody can even be blocked by attached QDs. All these facts can contribute significantly to the heterogeneity of the electrophoretic mobilites of immunoprobes, which negatively influence their separation resolution. In order to avoid this

problem we used monoclonal antibodies, which was earlier stated as a way to positively influence separation resolution [56].

In the next experiment, we studied how adding free CdTe QDs to solution will affect electrophoretic mobility and fluorescence intensity of QDs immunocomplex. Three different concentrations were used: 0.5, 0.1 and 0.01 mg/ml (Figure 18). Dependences of all three peaks on a QDs concentration is presented in Figure 19. We can clearly see that fluorescence intensity of free CdTe QDs peak increases progressively with increasing concentration of QDs. On the other hand, the adding of free QDs to a mixture after conjugation didn't provide any significant interaction of free QDs with conjugates and immunocomplex. There was no significant decreasing in peak area of QDs-Ab and immunocomplex peak with increasing of QDs concentration Figure 19. Same trend was stated by other authors [57].

In case when IgG was used, same dependence for peaks is noticed. The decrease in QDs and QDs-Ab and increase in QDs immunocomplex peak height or area is proportional to the amount of BSA and IgG present. The linear curve fitted equation and coefficient of determination represented are listed in Table 4.

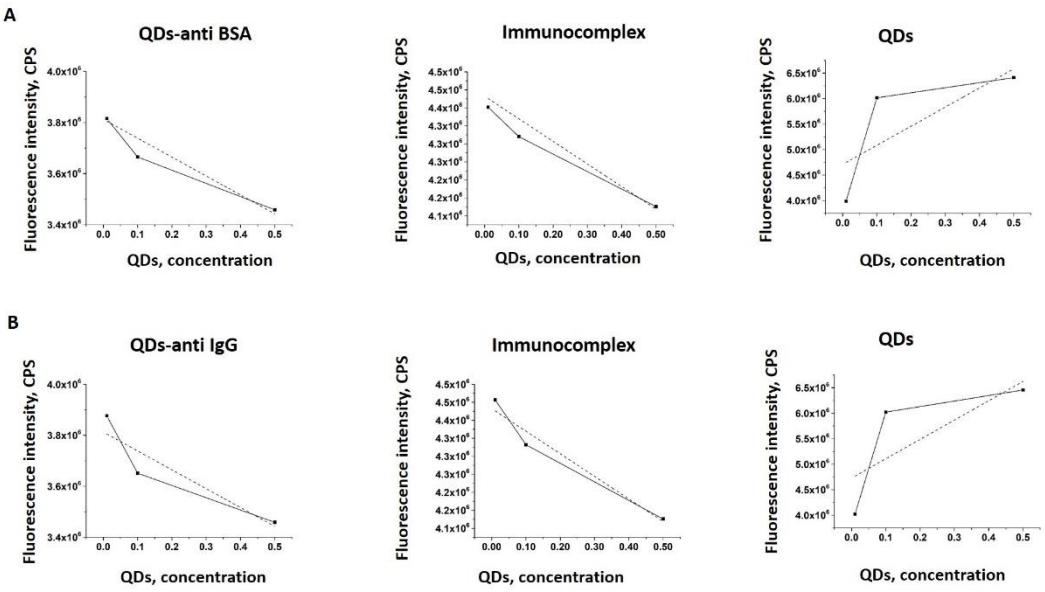

Figure 19 Dependence of pure QDs, QDs- antibody and immunocomplex peaks height on QDs concentration. A: Green QDs with BSA as an antigen, B: Orange QDs with IgG as an antigen.

Table 4 The linear curve fitted equation and their coefficient of determination

Sample	Coefficient of determination,R^2	Regression equation
Free green QDs	0.7514	$y = 3.7 \times 10^6 x + 4.7 \times 10^6$
Free orange QDs	0.7611	$y = 3.8 \times 10^6 x + 4.6 \times 10^6$
Green QDs-BSA	0.7125	$y = -7.3 \times 10^6 x + 3.9 \times 10^6$
Orange QDs-IgG	0.7042	$y = -7.4 \times 10^6 x + 3.8 \times 10^6$
Green QDs- immunocomplex	0.9162	$y = -6.2 \times 10^6 x + 4.5 \times 10^6$
Orange QDs- immunocomplex	0.9146	$y = -6.3 \times 10^6 x + 4.4 \times 10^6$

5.4 Influence of the buffer to a separation in on a chip CE

In order to keep the migration velocity of weak electrolyte components and the velocity of the EOF constant, the regulation of the pH is an important purpose of the BGE. In that way a stable and reproducible migration behavior of the sample components can be obtained. The larger mobilities of substance, the faster their electrophoretic migration the shorter time of analysis. However, even substance with zero effective mobilities may move in the capillary due to the EOF and the EOF is strongly dependent of the pH of the BGE used.

Generally, the most powerful selectivity agent in CE is pH, and therefore it requires special consideration and control. Often, adequate selectivity can be obtained by simply adjusting the pH, and then the other separation conditions can be optimized for further purposes such as separation speed.

The concentration of the BGE can play an important part in the resolution of a separation in electrophoresis, dependent on several aspects. If a constant voltage is applied over the capillary, the electric current will increase for higher concentrations of the BGE and this can cause extra peak broadening due to a strong increase in the Joule heat. Further a higher concentration of the BGE gives a lower mobility of the EOF and by this, fast and medium fast anions cannot be determined in the cathodic mode. Often there is a strong attraction force between positively charged analytes and the negatively charged wall of the silica capillary resulting in broad tailing sample zones. A high concentration of the BGE can decrease this adhesive behavior of the sample ions by a competitive adsorption of the co-ions of the BGE, thus increasing the resolution. The counter ions of the BGE can show attraction forces with analytes and this complexation can be stronger at a high concentration of the BGE.

To overcome this additional heat care must be taken in choosing buffer type and concentration. After set of experiment used 10 mM BBS buffer (borate buffered saline, pH = 9. 14) was chosen for experiments in this study. Using 10 mM BBS buffer and 3kV voltage avoids overheating of PDMS walls and fluid.

In order to increase mobility of analytes we tried to increase the pH value of the separation buffer. Usually, higher pH values would lead to similar increases in mobilities of both the immunocomplex and the antibody (Ab) hence could not improve the separation significantly. However, QD attached to the antibody could be a factor to influence the electrophoretic characteristics of the (Ab) and the complex in this study. The effect of QD on the Ab was greater than that on complex since both proteins, Ab and Ag, had contributions to the electrophoretic characteristics of the complex. Thus, the increase of buffer pH would amplify the effect of QD on the mobilities of the Ab and the complex. The mobility of the complex was expected to be influenced more by the buffer pH than that of the Ab peak.

The effects of buffer pH on the separation are shown in Figure 20. With the buffer of higher pH than 9.14, did not facilitate the formation of complex. The peak heights of the complex decreased at the pH 10.15 buffer and the peak of the complex disappeared eventually at pH 10.45. Optimal buffer pH value was set to 9.14 and the plate number.

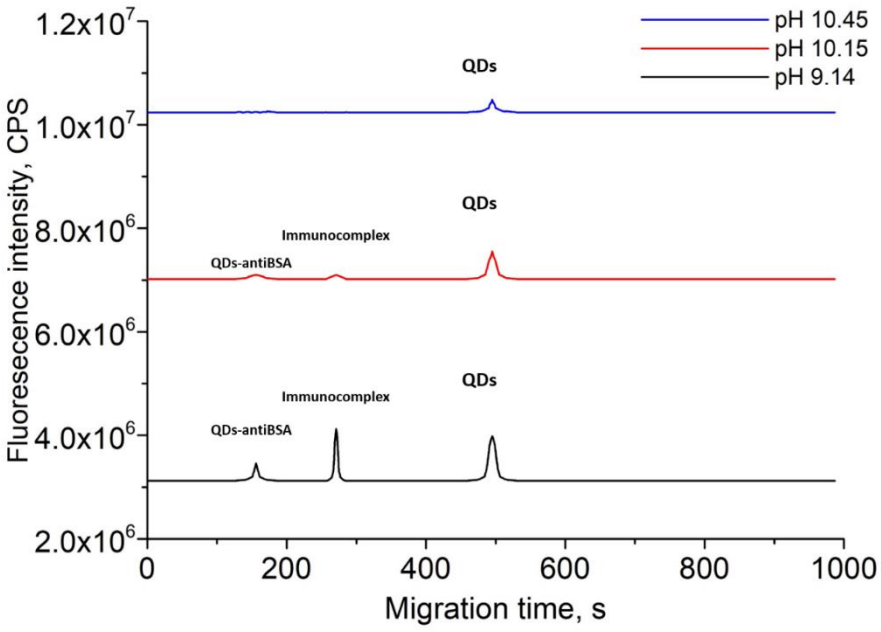

Figure 20 Effects of buffer pH values on a CdTe QDs antiBSA-BSA immunocomplex separation. Separation buffers: pH 9.14 (black), 10.15 (red) and 10.45 (blue).

5.5 CE on a chip immunoassay with both targets present

With the method presented in this chapter we were able to detect analytes conjugated with different size QDs at different emission wavelengths in a single run. Only one excitation

light source was used and two filter systems for different emission wavelengths. In our portable experiment set up, filter, LED and detector can be easily removed and replaced by other kind of equipment if needed for specific experiment. In Figure 21 electrophoretic behavior of a mixture of green QDs conjugated with immunocomplex BSA-anti BSA and orange QDs immunocomplex mIgG-anti mIgG run in experimental set up with two types of filter set up is presented.

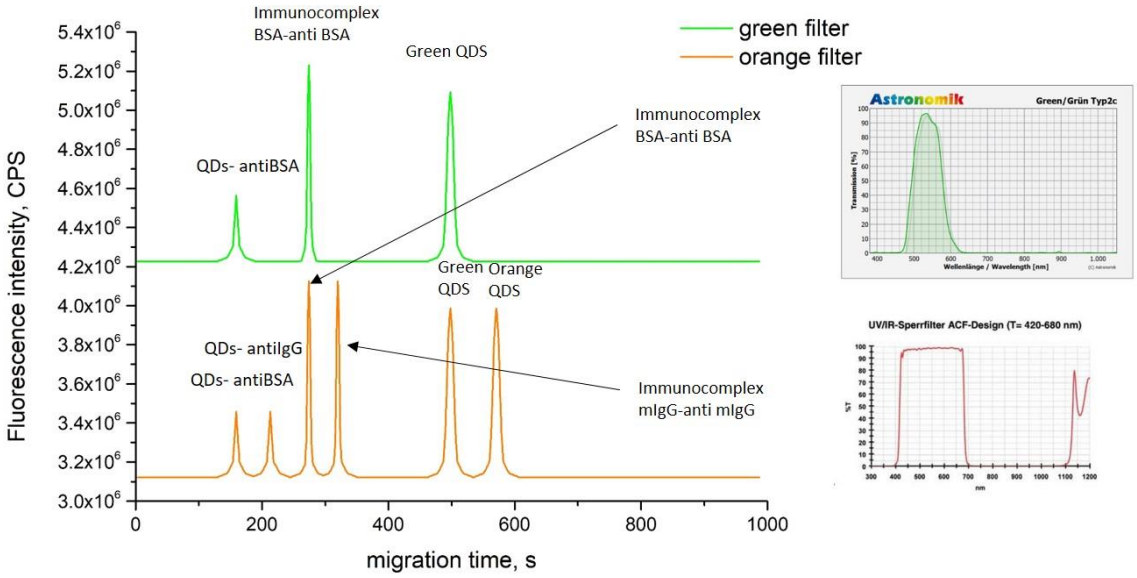

Figure 21 Electropherogram for separation of the mixture of two types of QDs 1. green CdTe–MPA QDs bioconjugated with BSA and 2. orange CdTe-MPA QDs bioconjugated with IgG. Using green and orange filter. Spectral characteristics of both filters are given on the left

The use of two filters with different wavelengths can distinguish the fluorescence coming from different size QDs. Using the 380 nm filter, fluorescence from orange QDs conjugates was completely filter out, as a result, only the fluorescence emission from green QDs and their conjugates is detected. Using the 420–680 nm high-pass optical filter, fluorescence from both orange and green QDs with their conjugates is detected. Using one excitation wavelength and two types of filter set up it was possible to detect two different immunocomplexes simultaneously.

6 CONCLUSION

QDs find a wide application in many different scientific filed, mostly in biology and medicine. Number of unique characteristic makes them especially interesting material for conjugation with biomolecules. Big issue in scientific world is toxicity of QDs. Due to increasing application of QDs in biology and medicine it is extremely important to better understand their interaction with biomolecules.

Biomodified QDs can be used in life science for drug delivery, luminescence tagging, implantable microdevices, and other. Further developing in this research field will depend on the understanding of specificity and capabilities of biomolecule–QD-coupling techniques and on the development of methods of characterization and separation of the conjugates. In this study, we successfully separated CdTe QDs bioconjugated with BSA using on-a-chip electrophoresis. Studying of quenching efficiency by measuring FL intensity showed that BSA is leading to a strong quenching effect of QD FL emission. Quenching effect depends on a coupling agent used to conjugate protein and it was the highest one when using EDC/sulfo-NHS.

In the work, we were able to get the quantitative detection of multiple antigen-antibody reaction on a single assay. Mixing two kinds of QDs bioconjugated with two different proteins and antibodies we were able to detect immunocomplex peaks with different areas which depends of concentration of QDs and antibody and antibody-antigen reaction. It is expected that CE immunoassays will continue to be explored for use in other clinical applications and to eventually mature into a method that is suitable for use in routine clinical laboratories.

The advantage of the work presented in this thesis is that it combines several improved techniques:

1. When using QDs instead of organic fluorophores a single light source can excite multicolor QDs without signal overlap
2. Using on a chip CE has its own advantages like simplicity, small sample and reagent requirements and high efficiency
3. When using portable experiment set up filter, LED and detector can be easily removed and replaced by other kind of equipment if needed for specific experiment.

Overall, the method developed can be applied to the determinations of other large bio-molecules in clinical and environmental applications. The adoption of this method should be further enhanced as advances continue to be made in the stability, precision and cost of CE systems for retinue chemical analysis.

REFERENCES

1. Mattoussi, H., G. Palui, and H.B. Na, *Luminescent quantum dots as platforms for probing in vitro and in vivo biological processes.* Advanced Drug Delivery Reviews, 2012. **64**(2): p. 138-166.
2. Tomczak, N., et al., *Designer polymer-quantum dot architectures.* Progress in Polymer Science, 2009. **34**(5): p. 393-430.
3. Pinaud, F., et al., *Advances in fluorescence imaging with quantum dot bio-probes.* Biomaterials, 2006. **27**(9): p. 1679-1687.
4. Chomoucka, J., et al., *Cell toxicity and preparation of streptavidin-modified iron nanoparticles and glutathione-modified cadmium-based quantum dots.* Procedia Engineering, 2010. **5**: p. 922-925.
5. Hoshino, A., et al., *Physicochemical Properties and Cellular Toxicity of Nanocrystal Quantum Dots Depend on Their Surface Modification.* Nano Letters, 2004. **4**(11): p. 2163-2169.
6. Morelli, E., et al., *Chemical stability of CdSe quantum dots in seawater and their effects on a marine microalga.* Aquatic Toxicology, 2012. **122–123**(0): p. 153-162.
7. Huang, X., et al., *Characterization of quantum dot bioconjugates by capillary electrophoresis with laser-induced fluorescent detection.* Journal of Chromatography A, 2006. **1113**(1–2): p. 251-254.
8. Mamedova, N.N., et al., *Albumin-CdTe nanoparticle bioconjugates: Preparation, structure, and interunit energy transfer with antenna effect.* Nano Letters, 2001. **1**(6): p. 281-286.
9. Wang, J.H., et al., *Bioconjugation of concanavalin and CdTe quantum dots and the detection of glucose.* Colloids and Surfaces a-Physicochemical and Engineering Aspects, 2010. **364**(1-3): p. 82-86.
10. Feng, H.T., et al., *Immunoassay by capillary electrophoresis with quantum dots.* Journal of Chromatography A, 2007. **1156**(1-2): p. 75-79.
11. Goldman, E.R., et al., *Conjugation of Luminescent Quantum Dots with Antibodies Using an Engineered Adaptor Protein To Provide New Reagents for Fluoroimmunoassays.* Analytical Chemistry, 2002. **74**(4): p. 841-847.
12. Pathak, S., M.C. Davidson, and G.A. Silva, *Characterization of the Functional Binding Properties of Antibody Conjugated Quantum Dots.* Nano Letters, 2007. **7**(7): p. 1839-1845.
13. Ji, X., et al., *(CdSe)ZnS Quantum Dots and Organophosphorus Hydrolase Bioconjugate as Biosensors for Detection of Paraoxon.* The Journal of Physical Chemistry B, 2005. **109**(9): p. 3793-3799.
14. Dwarakanath, S., et al., *Quantum dot-antibody and aptamer conjugates shift fluorescence upon binding bacteria.* Biochemical and Biophysical Research Communications, 2004. **325**(3): p. 739-743.
15. Shan, Y., et al., *NHS-mediated QDs-peptide/protein conjugation and its application for cell labeling.* Talanta, 2008. **75**(4): p. 1008-1014.
16. Jimenez-López, J., et al., *Automated determination of Rifamycins making use of MPA–CdTe quantum dots.* Journal of Luminescence, 2016. **175**: p. 158-164.
17. Wang, J., et al., *Probing Antigen-Antibody Interaction Using Fluorescence Coupled Capillary Electrophoresis.* International Journal of Molecular Sciences, 2013. **14**(9): p. 19146.
18. Narain, R., *Chemistry of Bioconjugates: Synthesis, Characterization, and Biomedical Applications*. 2013, USA: Wiley. 496.
19. Pathak, S., et al., *Hydroxylated quantum dots as luminescent probes for in situ*

hybridization. Journal of the American Chemical Society, 2001. **123**(17): p. 4103-4104.
20. Song, X.T., et al., *Highly efficient size separation of CdTe quantum dots by capillary gel electrophoresis using polymer solution as sieving medium.* Electrophoresis, 2006. **27**(7): p. 1341-1346.
21. Nandi, P. and S.M. Lunte, *Recent trends in microdialysis sampling integrated with conventional and microanalytical systems for monitoring biological events: A review.* Analytica Chimica Acta, 2009. **651**(1): p. 1-14.
22. Amundsen, L.K. and H. Siren, *Immunoaffinity CE in clinical analysis of body fluids and tissues.* Electrophoresis, 2007. **28**(1-2): p. 99-113.
23. Liu, D., et al., *Current developments and applications of microfluidic technology toward clinical translation of nanomedicines.* Advanced Drug Delivery Reviews, 2018. **128**: p. 54-83.
24. Chiem, N.H. and D.J. Harrison, *Microchip systems for immunoassay: an integrated immunoreactor with electrophoretic separation for serum theophylline determination.* Clinical Chemistry, 1998. **44**(3): p. 591-598.
25. Chiem, N. and D.J. Harrison, *Microchip-based capillary electrophoresis for immunoassays: Analysis of monoclonal antibodies and theophylline.* Analytical Chemistry, 1997. **69**(3): p. 373-378.
26. Fister, J.C., et al., *Counting single chromophore molecules for ultrasensitive analysis and separations on microchip devices.* Analytical Chemistry, 1998. **70**(3): p. 431-437.
27. Moser, A.C., C.W. Willicott, and D.S. Hage, *Clinical applications of capillary electrophoresis based immunoassays.* Electrophoresis, 2014. **35**(7): p. 937-955.
28. Sang, F.M., X.Y. Huang, and J.C. Ren, *Characterization and separation of semiconductor quantum dots and their conjugates by capillary electrophoresis.* Electrophoresis, 2014. **35**(6): p. 793-803.
29. Maryatiy, M., et al., *A fluorescence-based assay suitable for quantitative analysis of deadenylase enzyme activity.* Nucleic Acids Research, 2014. **42**(5).
30. Swartzman, E.E., et al., *A homogeneous and multiplexed immunoassay for high-throughput screening using fluorometric microvolume assay technology.* Analytical Biochemistry, 1999. **271**(2): p. 143-151.
31. Becker, S., et al., *Ultra-high-throughput screening based on cell-surface display and fluorescence-activated cell sorting for the identification of novel biocatalysts.* Current Opinion in Biotechnology, 2004. **15**(4): p. 323-329.
32. Resch-Genger, U., et al., *Quantum dots versus organic dyes as fluorescent labels.* Nature Methods, 2008. **5**(9): p. 763-775.
33. Doria, G., et al., *Noble metal nanoparticles for biosensing applications.* Sensors (Basel, Switzerland), 2012. **12**(2): p. 1657-1687.
34. Long, Z., et al., *Visual enantioselective probe based on metal organic framework incorporating quantum dots.* Microchemical Journal, 2013. **110**: p. 764-769.
35. Liskova, M., et al., *Conjugation reactions in the preparations of quantum dot-based immunoluminescent probes for analysis of proteins by capillary electrophoresis.* Analytical and Bioanalytical Chemistry, 2011. **400**(2): p. 369-379.
36. Tian, J.N., et al., *Controllable synthesis and cell-imaging studies on CdTe quantum dots together capped by glutathione and thioglycolic acid.* Journal of Colloid and Interface Science, 2009. **336**(2): p. 504-509.
37. Chopra, A., et al., *CdTe nanobioprobe based optoelectrochemical immunodetection of diabetic marker HbA1c.* Biosensors & Bioelectronics, 2013. **44**: p. 132-135.
38. Bubendorfer, A.J., et al., *Contamination of PDMS microchannels by lithographic molds.* Lab on a Chip, 2013. **13**(22): p. 4312-4316.
39. Roman, G.T., K. McDaniel, and C.T. Culbertson, *High efficiency micellar electrokinetic chromatography of hydrophobic analytes on poly(dimethylsiloxane) microchips.* Analyst, 2006. **131**(2): p. 194-201.

40. Thorslund, S. and F. Nikolajeff, *Instant oxidation of closed microchannels.* Journal of Micromechanics and Microengineering, 2007. **17**(4): p. N16-N21.
41. Filla, L.A., D.C. Kirkpatrick, and R.S. Martin, *Use of a Corona Discharge to Selectively Pattern a Hydrophilic/Hydrophobic Interface for Integrating Segmented Flow with Microchip Electrophoresis and Electrochemical Detection.* Analytical Chemistry, 2011. **83**(15): p. 5996-6003.
42. Vickers, J.A., M.M. Caulum, and C.S. Henry, *Generation of Hydrophilic Poly(dimethylsiloxane) for High-Performance Microchip Electrophoresis.* Analytical Chemistry, 2006. **78**(21): p. 7446-7452.
43. McDonald, J.C., et al., *Fabrication of microfluidic systems in poly(dimethylsiloxane).* Electrophoresis, 2000. **21**(1): p. 27-40.
44. Zhou, J.W., A.V. Ellis, and N.H. Voelcker, *Recent developments in PDMS surface modification for microfluidic devices.* Electrophoresis, 2010. **31**(1): p. 2-16.
45. Jai Kumar, B., D. Sumanth Kumar, and H.M. Mahesh, *A facile single injection Hydrothermal method for the synthesis of thiol capped CdTe Quantum dots as light harvesters.* Journal of Luminescence, 2016. **178**: p. 362-367.
46. Vicente, G. and L.A. Colon, *Separation of bioconjugated quantum dots using capillary electrophoresis.* Analytical Chemistry, 2008. **80**(6): p. 1988-1994.
47. Ryvolova, M., et al., *Glutathione modified CdTe quantum dots as a label for studying DNA interactions with platinum based cytostatics.* ELECTROPHORESIS, 2013. **34**(6): p. 801-808.
48. Vaishanav, S.K., et al., *Adsorption Kinetics and Binding Studies of Protein Quantum Dots Interaction: A Spectroscopic Approach.* Journal of Fluorescence, 2016. **26**(3): p. 855-865.
49. Ghali, M., *Static quenching of bovine serum albumin conjugated with small size CdS nanocrystalline quantum dots.* Journal of Luminescence, 2010. **130**(7): p. 1254-1257.
50. Ellappan, V., et al., *Interaction of digestive enzymes with tunable light emitting quantum dots: a thorough Spectroscopic investigation.* Luminescence, 2015. **30**(7): p. 978-989.
51. German, I. and R.T. Kennedy, *Rapid simultaneous determination of glucagon and insulin by capillary electrophoresis immunoassays.* Journal of Chromatography B, 2000. **742**(2): p. 353-362.
52. Phillips, T.M. and E.F. Wellner, *Analysis of inflammatory biomarkers from tissue biopsies by chip-based immunoaffinity CE.* Electrophoresis, 2007. **28**(17): p. 3041-3048.
53. Caslavska, J., D. Allemann, and W. Thormann, *Analysis of urinary drugs of abuse by a multianalyte capillary electrophoretic immunoassay.* Journal of Chromatography A, 1999. **838**(1-2): p. 197-211.
54. Heegaard, N.H.H. and R.T. Kennedy, *Identification, quantitation, and characterization of biomolecules by capillary electrophoretic analysis of binding interactions.* Electrophoresis, 1999. **20**(15-16): p. 3122-3133.
55. Pereira, M. and E.P. Lai, *Capillary electrophoresis for the characterization of quantum dots after non-selective or selective bioconjugation with antibodies for immunoassay.* Journal of Nanobiotechnology, 2008. **6**(1): p. 10.
56. Shimura, K. and B.L. Karger, *Affinity probe capillary electrophoresis: analysis of recombinant human growth hormone with a fluorescent labeled antibody fragment.* Analytical Chemistry, 1994. **66**(1): p. 9-15.
57. Kleparnik, K., et al., *Capillary electrophoresis immunoassays with conjugated quantum dots.* Electrophoresis, 2011. **32**(10): p. 1217-1223.

LIST OF FIGURES

LIST OF TABLES

AUTHORS PUBLICATIONS AND OTHER INPUTS

PUBLICATIONS:

PEJOVIČ SIMEUNOVIČ, J.; PEKÁRKOVÁ, J.; ŽÁK, J.; CHAMRADOVÁ, I.; HUBÁLEK, J. Studying of quantum dot luminescence quenching effect caused by covalent conjugation with protein. Monatshefte für Chemie, 2017, roč. 148, č. 11, s. 1901-1909. ISSN: 1434-4475.

KURZHALS, S.; SÜSS, M.; PEJOVIČ SIMEUNOVIČ, J.; VAN OOSTRUM, P.; REIMHULT, E.; ZIRBS, R. Crosslinking of floating colloidal monolayers. *Monatshefte für Chemie,* 2017, roč. 148, č. 8, s. 1539-1546. ISSN: 1434-4475.

SIMEUNOVIĆ, J. P.; GADJANSKI, I.; JANIĆIJEVIĆ, Ž.; JANKOVIĆ, M. M; BARJAKTAROVIĆ, M. M; JANKOVIĆ, N. Z; ČANTRAK Đ. S. Microfluidic Chip Fabrication for Application in Low-Cost DIY MicroPIV. In Proceedings of 5th International Conference on Advanced Manufacturing Engineering and Technologies. 1. Springer, Cham, 2017. s. 451-459. ISBN: 978-3-319-56430-2.

PEJOVIC SIMEUNOVIC, J.; HUBÁLEK, J. Separation and detection of bioconjugated quantum dots using on a chip electrophoresis. In Proceedings of the 22nd Conference STUDENT EEICT 2016. první. Brno: Vysoké učení technické v Brně, Fakulta elektrotechniky a komunikačních, 2016. s. 660-664. ISBN: 978-80-214-5350- 0.

PEJOVIC SIMEUNOVIC, J.; PEKÁRKOVÁ, J.; ŽAK, J.; HUBÁLEK, J. ON-A- CHIP ELECTROPHORESIS FOR THE CHARACTERIZATION OF QUANTUM DOTS BIOCONJUGATES. In CECE 2016, the 13 th International Interdisciplinary Meeting on Bioanalysis. Brno: Institute of Analytical Chemistry of the CAS, 2016. s. 211-214. ISBN: 978-80-904959-4-4.

PEJOVIC SIMEUNOVIC, J.; PEKÁRKOVÁ, J.; HUBÁLEK, J. Separation and detection of bioconjugated QDs in microfluidic devices using capillary electrophoresis. CEITEC PhD Retreat. 1. Brno: Masarykova univerzita, 2015. s. 109-109. ISBN: 978-80-210-7825- 3.

PRODUCTS:

ŽÁK, J.; SEDLÁČEK, J.; PEJOVIC, J.; PEKÁRKOVÁ, J.: HVElektroforezniZdroj; VN zdroj pro řízení kapilární elektroforézy. Technická 10, 0.66. URL: http://www.umel.feec.vutbr.cz/LabSensNano/products.aspx?id=91. (funkční vzorek)

PROJECTS:

GA16-11140S, Microfluidics-based Ultra Fast Differential Scaning Fluorometry for Drug Discovery (uDSF) start: 01.01.2016, end: 31.3.2017- research team member

Advanced nanotechnologies and materials, start: 01.01.2014, end: 31.12.2016

FOREIGN INTERNSHIP:

Doctoral internship (10.11.2014 - 19.12.2014. and 01.02.2015-31.07.2015.) at Universität für Bodenkultur Wien (BOKU), in Department of Nanobiotechnology (DNBT)